Contrasted geographical distribution of N_2 fixation rates and *nif*H phylotypes in the Coral and Solomon Seas (southwestern Pacific) during austral winter conditions

Sophie Bonnet, Martine Rodier, Kendra A. Turk-Kubo, Cyril Germineaud, Christophe E. Menkès, Alexandre Ganachaud, Sophie Cravatte, Patrick Raimbault, Ellen Campbell, Fabien Quéroué, et al.

AGU PUBLICATIONS

Global Biogeochemical Cycles

RESEARCH ARTICLE
10.1002/2015GB005117

Key Points:
- N_2 fixation is reported for the first time in the Solomon Sea and is among the highest of the ocean
- N_2 fixation rates are 20 times higher in the Solomon Sea compared with the Coral Sea
- UCYN-A/γ-24774A11 dominate in the Coral Sea; Trichodesmium/UCYN-B dominate in the Solomon Sea

Correspondence to:
S. Bonnet,
sophie.bonnet@ird.fr

Citation:
Bonnet, S., et al. (2015), Contrasted geographical distribution of N_2 fixation rates and *nif*H phylotypes in the Coral and Solomon Seas (southwestern Pacific) during austral winter conditions, *Global Biogeochem. Cycles*, *29*, 1874–1892, doi:10.1002/2015GB005117.

Received 16 FEB 2015
Accepted 2 OCT 2015
Accepted article online 5 OCT 2015
Published online 2 NOV 2015

Contrasted geographical distribution of N_2 fixation rates and *nif*H phylotypes in the Coral and Solomon Seas (southwestern Pacific) during austral winter conditions

Sophie Bonnet[1], Martine Rodier[2], Kendra A. Turk-Kubo[3], Cyril Germineaud[4], Christophe Menkes[5], Alexandre Ganachaud[4], Sophie Cravatte[1], Patrick Raimbault[1], Ellen Campbell[3], Fabien Quéroué[6], Géraldine Sarthou[6], Anne Desnues[1], Christophe Maes[7], and Gerard Eldin[4]

[1]Aix Marseille Université, CNRS/INSU, Université de Toulon, IRD, Mediterranean Institute of Oceanography UM 110, Marseille, France, [2]Ecosystèmes Insulaires Océaniens, Institut de Recherche pour le Développement-Université de la Polynésie Française-Institut Malarmé-Ifremer, Papeete, French Polynesia, [3]Department of Ocean Sciences, University of California, Santa Cruz, California, USA, [4]Institut de Recherche pour le Développement-Université de Toulouse III-CNRS-CNES, UMR5566-Laboratoire d'Etudes en Geophysique et Oceanographie Spatiale, Toulouse CEDEX, France, [5]Institut de Recherche pour le Développement-Sorbonne Universités (UPMC, Université Paris 06)-CNRS-MNHN, Laboratoire d'Océanographie et du Climat: Expérimentations et Approches Numériques, Nouméa CEDEX, New Caledonia, [6]Laboratoire des Sciences de l'Environnement Marin, UMR CNRS-IRD-UBO-IFREMER 6539/LEMAR/IUEM, Technopôle Brest Iroise, Place Nicolas Copernic, Plouzané, France, [7]Laboratoire de Physique des Océans, UMR 6523 CNRS-Ifremer-IRD-UBO, Centre Ifremer de Brest, Plouzané, France

Abstract Biological dinitrogen (N_2) fixation and the distribution of diazotrophic phylotypes were investigated during two cruises in the Coral Sea and the Solomon Sea (southwestern Pacific) during austral winter conditions. N_2 fixation rates were measurable at every station, but integrated (0–150 m) rates were an order of magnitude higher in the Solomon Sea (30 to 5449 μmol N m^{-2} d^{-1}) compared to those measured in the Coral Sea (2 to 109 μmol N m^{-2} d^{-1}). Rates measured in the Solomon Sea were in the upper range (100–1000 μmol N m^{-2} d^{-1}) or higher than rates compiled in the global MARine Ecosystem biomass DATa database, indicating that this region has some of the highest N_2 fixation rates reported in the global ocean. While unicellular diazotrophic cyanobacteria from group A (UCYN-A1 and UCYN-A2) and the proteobacteria γ-24774A11 dominated in the Coral Sea and were correlated with N_2 fixation rates ($p < 0.05$), *Trichodesmium* and UCYN-B dominated in the Solomon Sea and were correlated ($p < 0.05$) with N_2 fixation rates. UCYN-A were totally absent in the Solomon Sea. The biogeographical distribution of diazotrophs is discussed within the context of patterns in measured environmental parameters.

1. Introduction

Biological N_2 fixation is the conversion of the unreactive atmospheric N_2 into ammonia (NH_3) by diazotrophic (or N_2 fixing) organisms. At the global scale, new N introduced to the oceans by diazotrophic activity accounts for 140 ± 50 Tg of N every year [*Deutsch et al.*, 2007]. It is a major external source of N for the ocean, significantly larger than atmospheric and riverine sources [*Gruber*, 2004; *Codispoti et al.*, 2001]. N_2 fixing organisms thus act as "natural fertilizers," and contribute to sustaining primary productivity and carbon (C) export in oceanic environments [e.g., *Karl et al.*, 1997, 2012], especially in nutrient-poor (or oligotrophic) ecosystems.

This process is performed by a limited number of prokaryotes that have been shown to possess the *nif*H gene encoding the iron (Fe) protein of the nitrogenase enzyme [*Zehr et al.*, 1998, 2001]. They include photosynthetic cyanobacteria inhabiting the sunlit layer of the ocean, which have been the most intensively studied over the last decades. They also include heterotrophic bacteria [*Moisander et al.*, 2014; *Zehr et al.*, 1998; *Riemann et al.*, 2010; *Turk-Kubo et al.*, 2013], which are also present in aphotic waters [*Fernandez et al.*, 2011; *Hewson et al.*, 2007], where they have been seen to account for up to 90% of N_2 fixed throughout the depth-integrated water column [*Bonnet et al.*, 2013] in the tropical Pacific ocean. These latter organisms are currently the subject of numerous studies in order to quantify their contribution to global N_2 fixation.

A recent international collaborative effort performed in the framework of the MARine Ecosystem biomass DATa (MAREDAT) initiative [*Buitenhuis et al.*, 2012] led to the construction of a global database on biological

N_2 fixation [*Luo et al.*, 2012] compiling about 12,000 direct field measurements of N_2 fixation rates and cell counts of diazotrophs in the global ocean. It provides very useful information regarding spatial patterns of diazotrophic activity and diversity at the global scale. It reveals that geometric means of depth-integrated N_2 fixation rates in the Pacific Ocean are higher than in the Atlantic Ocean. In both ocean basins, rates are higher in the northern hemisphere compared to the southern hemisphere. However, as stated by *Luo et al.* [2012] and *Luo et al.* [2014], there are still vast oceanic areas where diazotrophic activity has not yet been measured, and in particular there is very little data from the subtropical southern Pacific, South Atlantic, and Indian Oceans. Only four studies [*Garcia et al.*, 2007; *Moisander et al.*, 2010; *Raimbault and Garcia*, 2008; *Bonnet et al.*, 2008] are reported in the database for the subtropical southern Pacific compared to 13 studies [*Luo et al.*, 2012] for the subtropical northern Pacific. Moreover, the few data sets available for the subtropical southern Pacific reveal a large variability of biogeochemical conditions in two larger regions. First, the ultra-oligotrophic South Pacific subtropical gyre is characterized by low N_2 fixation rates (60 ± 30 μmol N m^{-2} d^{-1}, [*Raimbault and Garcia*, 2008]) and low numbers of diazotrophs, mainly affiliated to heterotrophic proteobacteria and prymnesiophyte-associated unicellular diazotrophic cyanobacteria from group A (UCYN-A) [*Halm et al.*, 2012; *Bonnet et al.*, 2008]. In contrast, the oligotrophic western tropical and subtropical South Pacific (hereafter SW Pacific) is characterized by high N_2 fixation rates (151 to 703 μmol N m^{-2} d^{-1}, [*Garcia et al.*, 2007]) and high abundances of *Trichodesmium*, UCYN-A, UCYN-B, and γ-proteobacteria [*Moisander et al.*, 2014, 2010]. This increasing longitudinal east-west gradient has recently been confirmed by *Shiozaki et al.* [2014]. Farther north in the western tropical/equatorial Pacific, two cruises reported extremely high rates of N_2 fixation in the Arafura Sea between Australia and Papua New Guinea (PNG) (4000 μmol N m^{-2} d^{-1}, [*Montoya et al.*, 2004]) and in the Vitiaz strait east of PNG (11,900 μmol N m^{-2} d^{-1}, [*Bonnet et al.*, 2009]). The SW Pacific is thus considered to be one of the highest areas of global N_2 fixation [*Capone et al.*, 1997; *Sohm et al.*, 2011a], but there is very little data from vast regions such as the Coral Sea [*Moisander et al.*, 2010] and the Solomon Sea has never been studied. However, these seas play a key role in the redistribution of water to the equator [*Kessler and Cravatte*, 2013; *Ganachaud et al.*, 2014], and N_2 fixation in the Coral and Solomon Seas may impact N inventories and primary productivity farther north in the equatorial Pacific. Moreover, most of the previous studies characterizing N_2 fixation rates in the SW Pacific have sampled austral summer conditions (October to April), which is considered the favorable season for N_2 fixation [*Garcia et al.*, 2007], but the patterns of distribution, abundance, activity and diversity of diazotrophs in this region remain poorly understood during austral winter conditions (May to September).

In the present study, we report data from two cruises in the critically undersampled Coral and the Solomon Seas during austral winter conditions (July to September) in order to answer the following questions: (i) What is the range of N_2 fixation rates along physicochemical gradients during these two cruises?; (ii) Who are the major diazotroph phylotypes in the region and which environmental factors control their distribution?; and (iii) What is the potential biogeochemical impact of N_2 fixation in this region?

2. Materials and Methods

This study was carried out during two cruises performed during austral winter conditions: the Pandora cruise (R/V *Atalante*, June to July 2012), which transited north from Noumea along 163°E and across the Solomon Sea (Figure 1a), and the Bifurcation cruise (R/V *Alis*, September 2012), which transited from Noumea (New Caledonia) to the northeast region of the Coral Sea (Figure 1b).

2.1. Acoustic Doppler Current Profiler (ADCP) Data Acquisition

ADCP current data were continuously recorded during both cruises using ship-mounted RDI equipment and processed using the CODAS software (http://currents.soest.hawaii.edu/); in the present study only data from Pandora OS150 ADCP will be used, consisting of 10 min averaged profiles of 8 m vertical bins, with the shallowest bin at 16 m depth.

2.2. Temperature, Nutrients, and Chlorophyll Measurements

Surface temperature and salinity were continuously recorded during both cruises using the shipboard thermosalinograph. Data were calibrated following the Global Ocean Surface Underway Data procedure and were taken from the Coriolis database. Thermosalinograph salinity was verified to be very close to measured conductivity-temperature-depth (CTD) salinities at 5 m depth (near the water intake for the TSG).

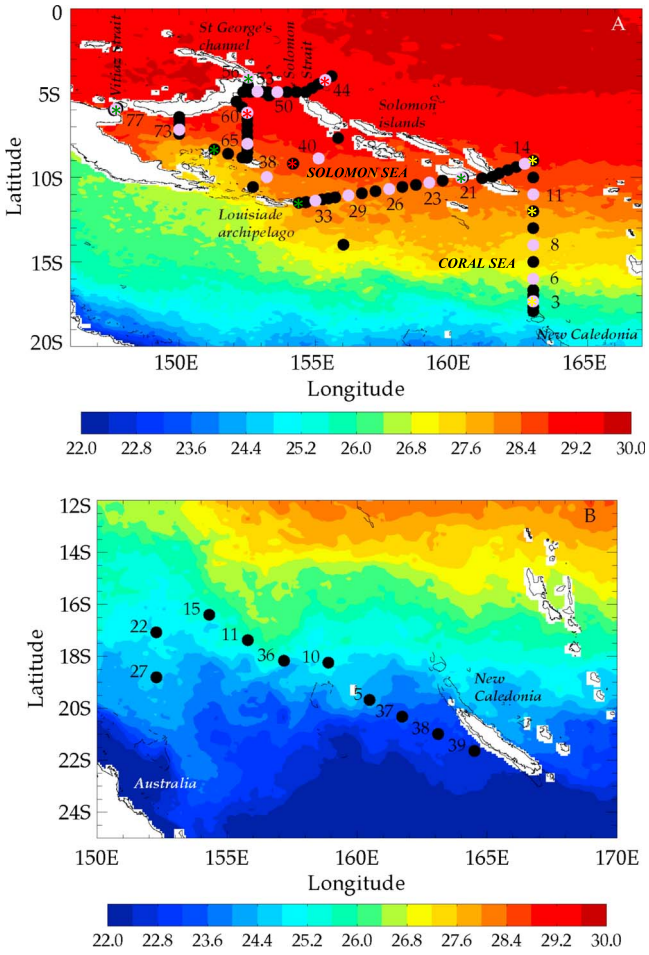

Figure 1. Sampling stations superimposed on a composite sea surface temperature (SST, °C) plot for the study period. (a) Pandora cruise (Solomon Sea, R/V *Atalante*, July 2012; black dots: hydrological stations, pink dots: biogeochemical stations). Asterisks indicate the stations where DFe concentrations were measured (green: Solomon Sea coastal stations; red: Solomon Sea offshore stations, i.e., located at more than 120 km from the coast; yellow: Coral Sea stations. (b) Bifurcation cruise (Coral Sea, R/V *Alis*, September 2012). Daily sea surface temperature (SST, °C) was obtained from the group for high-resolution SST (www.ghrsst.org) at a 1/12° spatial resolution.

To detect large salinity gradients, the 5 min salinity data were regridded onto a 2 km grid along the ship track, and gradients stronger than 0.005 practical salinity unit (psu) km^{-1} were selected.

CTD profiles were performed at 40 stations during the Bifurcation cruise (10 are reported here) and 83 stations during the Pandora cruise [*Eldin et al.*, 2013] (Figure 1). Vertical profiles of temperature, salinity, oxygen, and fluorescence were obtained using a Seabird 911 plus CTD equipped with a Wetlabs ECO-AFL/FL (Bifurcation) and Chelsea Aqua 3 (Pandora) fluorometer. Seawater samples for quantifying NO_x [nitrite (NO_2^-) + nitrate (NO_3^-)] and phosphate (PO_4^{3-}) concentrations were collected in acid-washed polyethylene bottles using a rosette equipped with 12 L Niskin bottles. Nutrient concentrations were determined using standard colorimetric techniques [*Aminot and Kerouel*, 2007] on a Bran Luebbe AA3 autoanalyzer. Detection limits for the procedures were 0.02 to 0.05 μmol L^{-1} for NO_x and 0.01 to 0.083 μmol L^{-1} for PO_4^{3-}. No PO_4^{3-} data are available from stations 1 to 18 during the Pandora cruise due to technical problems. Samples for dissolved iron (dFe) concentration measurements were collected from Go-Flo bottles using slight N_2 overpressure and filtration through 0.2 μm filter cartridges (Sartrobran-300, Sartorius). They were acidified to pH 2.0 with ultrapur® hydrochloric acid (HCl, Merck) and analyzed by flow injection with chemiluminescence detection as described in *Sarthou et al.* [2007]. Samples for Chl *a* concentrations were collected in 0.55 L flasks, filtered onto GF/F Whatman filters, deep frozen (−80°C) and analyzed onshore during the Bifurcation cruise and on board during the Pandora cruise. Chl *a* concentrations were determined after extraction with methanol [*Herbland et al.*, 1985] using a Turner Design fluorometer equipped with the Chl *a* extracted acidification module (module a 7200–040) and calibrated with pure Chl *a* standard (Sigma). For each cruise, the CTD in situ fluorescence data were fitted to the Chl *a* data from fluorometry measurements using a linear least squares regression.

2.3. Vertical Profiles of N_2 Fixation

Rates of N_2 fixation were measured at 10 stations during the Bifurcation cruise and at the 18 stations selected for biogeochemical analysis during the Pandora cruise (Figure 1). During the Bifurcation cruise, individual samples for N_2 fixation rate determination were collected at five depths between 0 and 200 m, corresponding to 0.1%, 3%, 15%, 35%, and 50% surface irradiance levels. During the Pandora cruise, four fixed depths (5 m, 50 m, 100 m, and 150 m) were sampled to fulfill the physical and geochemical parameter sampling requirements. The $^{15}N_2$ tracer method [*Montoya et al.*, 1996a] was used for both cruises: water samples were

dispensed into acid-leached 4.5 L polycarbonate bottles closed with septa and spiked with 4 mL $^{15}N_2$ (99 % Cambridge isotopes) via a gas-tight syringe and 1 mL of an 80 g L^{-1} $NaH^{13}CO_3$ solution (99 % Cambridge Isotopes). Each bottle was shaken 30 times to fragment the $^{15}N_2$ bubble and facilitate its dissolution. A recent study [*Dabundo et al.*, 2014] reports potential contamination of commercial $^{15}N_2$ gas stocks with ^{15}N-enriched ammonium, NO_3^- and/or NO_2^-, and nitrous oxide. The $^{15}N_2$ Cambridge isotope stocks analyzed contained low concentrations of ^{15}N contaminants, and the potential overestimated N_2 fixation rates modeled using this contamination level would range from undetectable to 0.02 nmol N L^{-1} d^{-1}. These rates are in the lower end of the range of rates measured in this study, and we thus considered that this issue did not affect the results reported here.

Bottles were then incubated for 24 h in on-deck incubators at irradiances corresponding to the sampling depth using screening and cooled with circulating surface seawater. After incubation, half of each 4.5 L was filtered under low vacuum pressure (<100 mm Hg) onto precombusted (4 h at 450°C) GF/F filters (25 mm diameter, 0.7 μm nominal porosity) for "bulk" N_2 fixation determination. The remaining volume was prefiltered onto 10 μm polycarbonate filters and collected onto precombusted GF/F filters for analysis of the pico and nanoplanktonic (<10 μm) N_2 fixation. Filters were stored at −20°C until the end of each cruise then dried for 24 h at 60°C and stored until mass spectrometric analysis.

During both cruises, an extra 2.2 L bottle was collected at the upper depth of the profile, spiked with $^{15}N_2$, and immediately filtered in order to determine the initial background $\delta^{15}N$ in the particulate organic N for calculations of N_2 fixation rates.

2.4. Mass Spectrometric Analyses

The particulate N (PN) and C (PC) content, ^{15}N isotopic, and ^{13}C enrichment analyses of each filter were performed by continuous-flow isotope ratio mass spectrometry using an Integra-CN mass spectrometer as described in *Bonnet et al.* [2011], *Raimbault and Garcia* [2008] and *Montoya et al.* [1996b]. The accuracy of the system was verified every 10 samples using reference material (International Atomic Energy Agency (IAEA), Analytical Quality Control Services). Before sample analysis, we checked the linearity of ^{15}N at. % as a function of increasing particulate N masses on IAEA reference material. ^{15}N at. % was linear (Fisher test, $p < 0.01$) between 0.20 and 10.00 μmol N, which is within the range of particulate N measured in all our samples. Detection and quantification limits for PN were 0.36 and 0.80 μmol N, respectively. The ^{13}C data are not shown in this paper but are used only to calculate the N demand of total primary productivity. In order to determine areal rates, N_2 fixation measurements were depth integrated using a conventional trapezoid procedure.

2.5. Quantification of Diazotrophs

Abundances of targeted diazotrophic phylotypes were determined using quantitative polymerase chain reaction (PCR) (qPCR) targeting the *nif*H gene. Samples for DNA were collected from Niskin bottles at the same depths and same stations as samples for N_2 fixation. First, 1.2 to 2.3 L of water was filtered through 10 μm (Osmonics) and next through 0.2 μm Supor (Pall-Gelman) filters using gentle peristaltic pumping and immediately flash frozen in liquid N_2. All filters were stored at −80°C thereafter. DNA was extracted from both 10 and 0.2 μm filters using the Qiagen DNeasy kit (Valencia, CA, USA), with protocol modifications described in [*Moisander et al.*, 2008] to optimize cell disruption using multiple freeze/thaw cycles, agitation via bead beating, and proteinase K digestion. The column purification and elution steps were automated using a QIACube (Qiagen). Quality and quantity of extracted DNA were assessed using a Nanodrop ND-1000 (Thermo Scientific, Waltham, MA).

The abundance of the following eight keystone diazotrophic phylotypes was determined using Taqman® qPCR assays: unicellular cyanobacterial groups A1 (UCYN-A1; [*Church et al.*, 2005a]), A2 (UCYN-A2; [*Thompson et al.*, 2014]), B (UCYN-B or *Crocosphaera* spp.; [*Moisander et al.*, 2010]), and C (UCYN-C; [*Foster et al.*, 2007]); the filamentous, colonial cyanobacteria *Trichodesmium* spp. [*Church et al.*, 2005a], *Richelia* associated with both *Rhizosolenia* (RR or het-1; [*Church et al.*, 2005a]) and *Hemiaulus* (HR or het-2; [*Foster et al.*, 2007]) diatoms, as well as a heterotrophic phylotype of gamma proteobacteria (γ-24474A11; [*Moisander et al.*, 2008]). Only surface samples from both Bifurcation and Pandora cruises were screened for the presence of UCYN-C. Protocols used for the generation of recombinant plasmid standards, as well as the qPCR reaction conditions and thermocycling parameters are described in detail by *Goebel et al.* [2010]. All samples were screened for

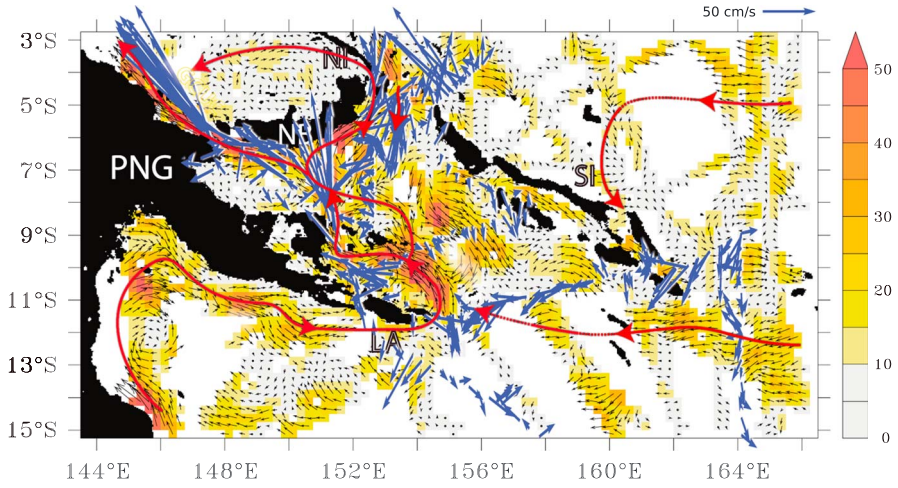

Figure 2. Mean near-surface layer (20–100 m) currents compiled from more than 20 years of shipboard acoustic Doppler current profiler data (adapted from *Cravatte et al.* [2011]). Colors represent the mean velocity amplitude in cm s^{-1}. Grid points with no data are blanked. Main surface currents deduced from *Cravatte et al.* [2011] and other publications are schematically represented by the red arrows. Superimposed in blue arrows are hourly averaged near-surface (16–24 m) current vectors along Pandora cruise ship track from OS150 shipboard ADCP. Scale bar is in the upper right corner. Rotating vectors during fixed stations (e.g., at both ends of southern section or south of St. George's Channel) are evidence of strong tidal currents.

inhibition using a spike of UCYN-A1 standard at 10^5 *nif*H copies reaction^{-1}. No inhibition was detected in Pandora cruise DNA extracts, but nearly all Bifurcation cruise DNA extracts were inhibited; therefore extracts were diluted 1:10 prior to use as template in qPCR reactions. For Pandora cruise samples, the limit of detection (LD) and limit of quantitation (LQ) ranged between 10–85 and 85–340 *nif*H copies L^{-1}, respectively. Results that fell between the LD and LQ for each sample were designated as detected not quantified. For Bifurcation cruise samples, the LD and LQ ranged between 106–136 and 851–1092 *nif*H copies L^{-1}, respectively. For visualization of *nif*H-based abundance data, data from the two size fractions were summed and log transformed as log10 (*nif*H copies L^{-1} + 1).

2.6. Statistical Analyses

To examine the potential relationship between N_2 fixation, *nif*H-based abundances of diazotrophs, and environmental parameters, Pearson's correlation coefficients were calculated and tested between each variable of interest (degree of freedom = $n - 2$, $\alpha = 0.05$ or 0.01; Tables 2 and 3). The dFe concentrations in and out of the Solomon Sea were compared using a two-tailed nonparametric mean comparison test (degree of freedom = $n - 2$, $\alpha = 0.05$, unpaired samples).

3. Results

3.1. Mean Circulation

The circulation in the Coral and Solomon Seas is relatively well known [*Ceccarelli et al.*, 2013; *Ganachaud et al.*, 2014; [*Kessler and Cravatte*, 2013]; *Cravatte et al.*, 2011]. The main feature is the westward flowing South Equatorial Current (SEC) that enters the Coral Sea between New Caledonia and Solomon Islands and redistributes waters toward the South Pole and the equator through the Solomon Sea. Within the Coral Sea, the broad SEC interacts with the topography to split and form narrow jets; small intense eddies are observed at the surface in late winter during the season of the Bifurcation cruise [*Hristova et al.*, 2014]. As shown schematically in Figure 2, waters in the surface layer enter the Solomon Sea mainly through the intense western boundary current on its western side and through the Solomon Strait. They exit through three narrow passages: Vitiaz Strait, St. George's Channel, and Solomon Strait. During the Pandora cruise, observed surface currents through Vitiaz Strait were particularly strong. The Solomon Sea is characterized by highly variable currents and strong mesoscale and submesoscale variability [*Djath et al.*, 2014; *Gourdeau et al.*, 2014; *Hristova et al.*, 2014]. Thus, instantaneous measurements made during this cruise are assumed to have been influenced by simultaneous mesoscale and submesoscale structures.

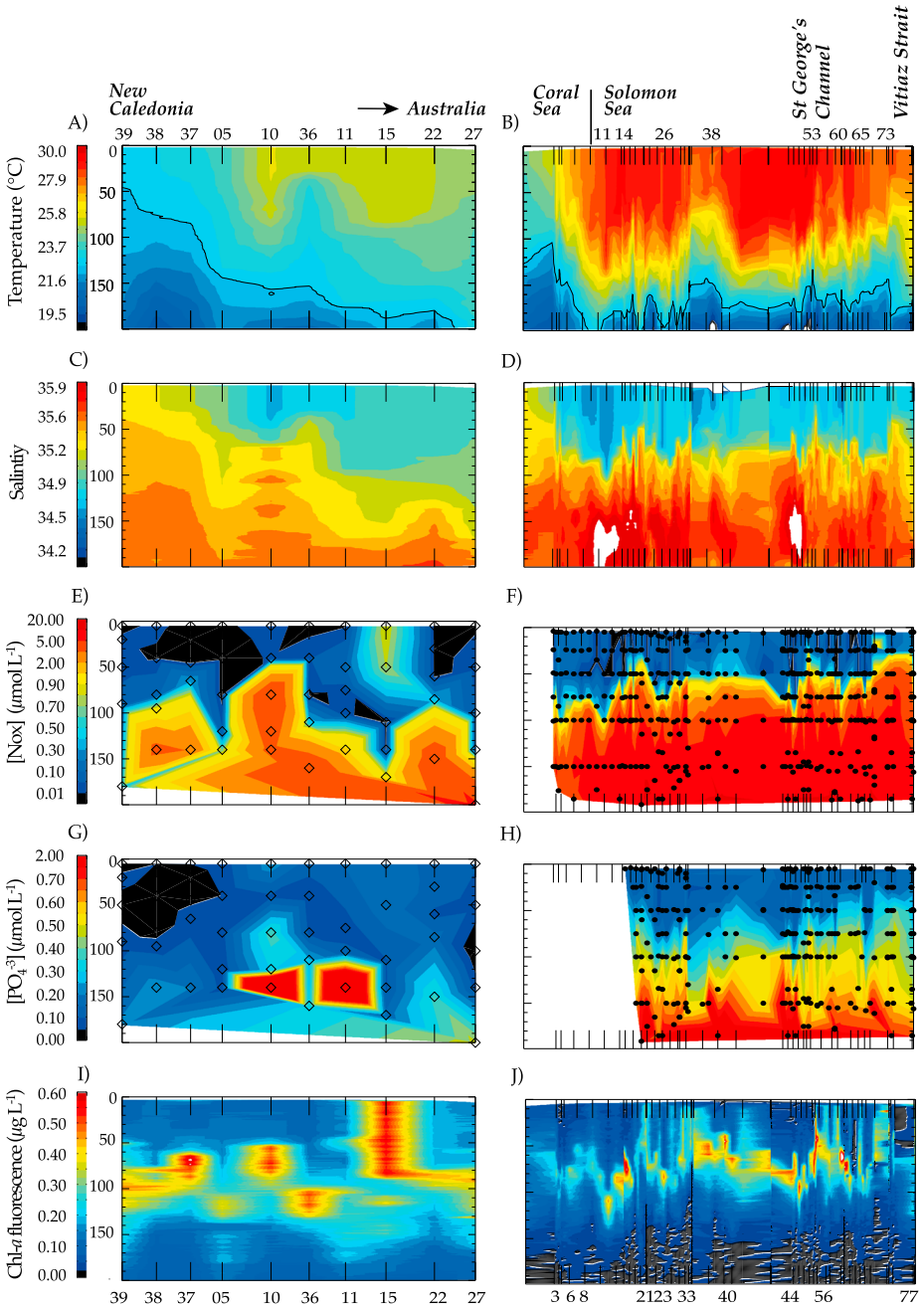

Figure 3. Horizontal and vertical distributions of physicochemical parameters during the (left) Bifurcation cruise and the (right) Pandora cruise: (a and b) temperature (°C), (c and d) salinity, (e and f) NO_x concentrations (µmol L^{-1}), (g and h) PO_4^{3-} concentrations (µmol L^{-1}), and (i and j) Chlorophyll *a* fluorescence (µg L^{-1}). Station numbers are reported on the top and bottom of panels.

3.2. Environmental Conditions

The transect performed at the end of austral winter in the Coral Sea (Bifurcation cruise) was characterized by a south-north sea surface temperature (SST) gradient with SSTs ranging from ~22.8–23.6°C at the southernmost stations around 21.5°S (nearest New Caledonia) to up to 26.2°C at the southern edge of the warm pool (station 11) (Figures 1b and 3a). The Pandora cruise took place earlier in the austral winter, when SSTs were cooler near New Caledonia, but since all Pandora cruise stations were located north of 19°S, the range of SST (25.3–29.6°C) measured over the Pandora cruise was regularly higher than during the Bifurcation cruise (Figures 1a and 3b).

The Bifurcation transect bordered a region with relatively deep thermoclines (~170–220 m) at stations 10–27 (thermocline depth was approximated by the depth of the 22°C isotherm, black curve in Figure 3a) and low-salinity waters compared to the eastern part of the transect (stations 37–39). During the transit back toward New Caledonia, the thermocline was shallower (up to 50 m at station 39) and the salinity increased (Figure 3c). Overall, the mixed layer structure reflected these variations with deep and warm temperatures up to station 27 representative of warm pool waters and with cooler waters close to New Caledonia (stations 37–39).

During the Pandora cruise, the depth of the thermocline at stations 4–37 was 180 m due to an anticyclonic (downwelling favorable, not shown) structure centered on 15°S/155°E. The thermocline then progressively shallowed with the transit north toward the Solomon Sea (stations 37–79) (Figure 3b). With the exception of the first two stations located near New Caledonia, the sampled water masses were representative of warm pool waters with a deep mixed layer and warm surface temperatures.

During the Bifurcation cruise, surface waters were depleted in NO_x (Figure 3e), with concentrations close or below the detection limit of conventional micromolar methods (~0.02 $\mu mol\,L^{-1}$). The NO_x-depleted layer varied from 50 m down to 150 m during the cruise. A particular feature was observed at station 15, where higher NO_x concentrations (~0.90 $\mu mol\,L^{-1}$) were measured in the 0–50 m upper layer. During the Pandora cruise, the NO_x-depleted layer (Figure 3f) depth was around 50–70 m except at the stations near the coast on each side of the southern entrance of the Solomon Sea (stations 21 and 33–34), where it was found at 30–40 m. Following a similar pattern, the depleted layer was also shallower in the St. George's Channel (stations 53–56) and in the Vitiaz Strait (station 77), leading to some near- surface NO_x enrichments up to 0.30 $\mu mol\,L^{-1}$.

PO_4^{3-} concentrations in the 0–50 m layer were always above 0.05 $\mu mol\,L^{-1}$ during the Bifurcation cruise (Figure 3g) except near the western coast of New Caledonia (stations 5 and 37 to 39), where surface PO_4^{3-} concentrations were as low as 0.02 $\mu mol\,L^{-1}$ (station 38). The highest surface PO_4^{3-} concentrations were measured at station 10 reaching 0.23 $\mu mol\,L^{-1}$. During the Pandora cruise, they were always above 0.08 $\mu mol\,L^{-1}$ (Figure 3h), and as described above for NO_x, the highest surface concentrations were measured at the southern entrance of the Solomon Sea and in the St. George's Channel (0.15–0.16 $\mu mol\,L^{-1}$). The NO_x:PO_4^{3-} molar ratios at ~150 m were 7 and 12, respectively, during Bifurcation and Pandora cruises, suggesting that primary productivity sustained by the supply of deep nutrients was N limited with respect to P at the time of sampling.

During the Bifurcation cruise, Chl *a* concentrations based on fluorescence data calibrated with chlorophyll ranged from 0.07 to 0.63 $\mu g\,L^{-1}$ over the 0–200 m layer during (Figure 3i). The deep chlorophyll maximum (DCM) was located between 50 and 125 m except around 154°E (station 15), where Chl *a* concentrations were uniformly high ($>$0.5 $\mu g\,L^{-1}$) over the 0–75 m layer, which is consistent with the relatively high NO_x concentrations (~0.9 $\mu mol\,L^{-1}$) reported in the 0–50 m upper layer at this station. During the Pandora cruise (Figure 3j), Chl *a* concentrations ranged from 0.05 to 0.73 $\mu g\,L^{-1}$. The DCM was mostly located between 50 and 100 m, but relatively high concentrations (between 0.23 and 0.30 $\mu g\,L^{-1}$) were occasionally measured in surface waters near the coasts, for instance, at both sides of the entrance of the Solomon Sea (stations 21, 34, and 36), near New Ireland (station 53), in the St. George's Channel (station 56), near New Britain (station 58), and in the Vitiaz Strait (station 77).

3.3. N_2 Fixation Rates

During both cruises, N_2 fixation rates were measurable at every station. The overall range of bulk rates was from the detection limit (DL) to 2.8 $nmol\,N\,L^{-1}\,d^{-1}$ during the Bifurcation cruise and from DL to 89.5 $nmol\,N\,L^{-1}\,d^{-1}$ during the Pandora cruise.

On the Bifurcation cruise, the highest rates were measured in surface waters at the three easternmost stations (stations 37–39) located close to New Caledonia and at 50 m at the northernmost station (station 15) which was located at the southern edge of the warm pool (Figure 4a). Most of the activity took place in the 0–50 m layer, but rates were also measurable down to 150 m (0.02–0.5 $nmol\,N\,L^{-1}\,d^{-1}$). Size fractionation experiments indicate that 70% of measured N_2 fixation was associated with the $<$10 μm size fraction (Figure 4b), and N_2 fixation in this fraction followed the same vertical pattern as for bulk N_2 fixation.

On the Pandora cruise, N_2 fixation rates were 20 times higher (significantly $p < 0.05$) than those measured on the Bifurcation cruise (Figure 5a). The lowest rates were measured along the 163°E transection in the Coral

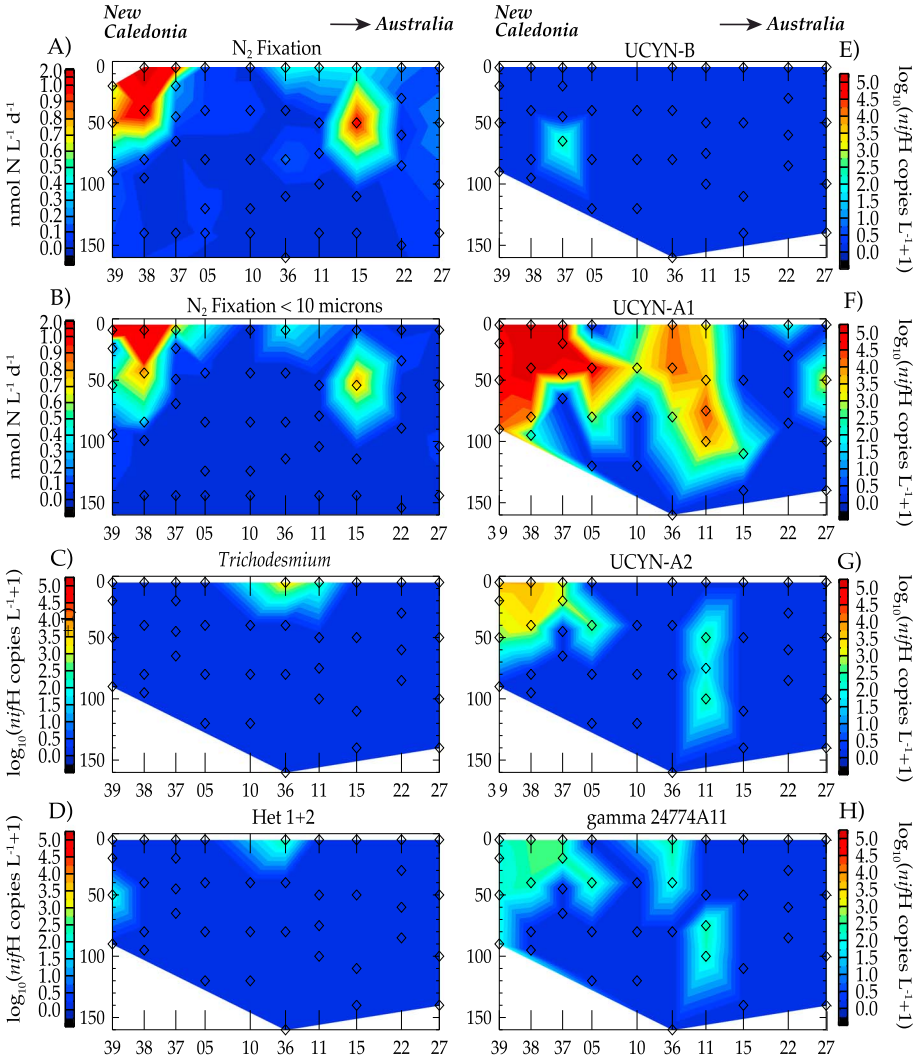

Figure 4. Horizontal and vertical distributions of N_2 fixation rates and diazotrophs during the Bifurcation cruise (R/V *Alis*). (a) Bulk N_2 fixation rates (nmol N L^{-1} d^{-1}), (b) N_2 fixation rates in fraction <10 μm (nmol N L^{-1} d^{-1}), (c) *Trichodesmium*, (d) Het-1 + Het-2, (e) UCYN-B, (f) UCYN-A1, (g) UCYN-A2, (h) γ-2474A11 abundances reported in log10 (*nif*H copies L^{-1} + 1). Station numbers are reported at the bottom of each panels.

Sea (stations 3, 6, 8, and 11; range DL–1.0 nmol N L^{-1} d^{-1}) and increased in the Solomon Sea (stations 21 to 77; range DL–89.5 nmol N L^{-1} d^{-1}). The highest rates over the cruise were measured in the St. George's Channel (station 56), where they reached 89.5 nmol N L^{-1} d^{-1} in surface waters but were still high at 150 m at 20.1 nmol N L^{-1} d^{-1}. High rates were also measured in surface waters at the southern entrance of the Solomon Sea (stations 23, 26, and 29, ranging from 8.7 to 15.3 nmol N L^{-1} d^{-1}), in the Vitiaz Strait (stations 73 and 77, ranging from 9.1 to 15.7 nmol N L^{-1} d^{-1}), and in the Solomon Strait (stations 44 and 50, ranging from 1.7 to 12.4 nmol N L^{-1} d^{-1}). In contrast, results from the Bifurcation cruise, size fractionation experiments (Figure 5b) indicate that the majority (65%) of N_2 fixation was associated with the >10 μm fraction over the whole transect, with only 35% of N_2 fixation being associated with the pico and nanoplanktonic size fraction (<10 μm fraction). The exception to this pattern is at station 56 (St. George's Channel), where more than 60% of the total N_2 fixation was associated with the <10 μm fraction.

When considering data from both cruises together, integrated rates over 0–150 to 0–200 m (Table 1) ranged from 2 to 109 μmol N m^{-2} d^{-1} in the Coral Sea (average 30 ± 33 μmol N m^{-2} d^{-1}) and from 30 to 5449 μmol N m^{-2} d^{-1} in the Solomon Sea (average 624 ± 1360 μmol N m^{-2} d^{-1}) (Table 1).

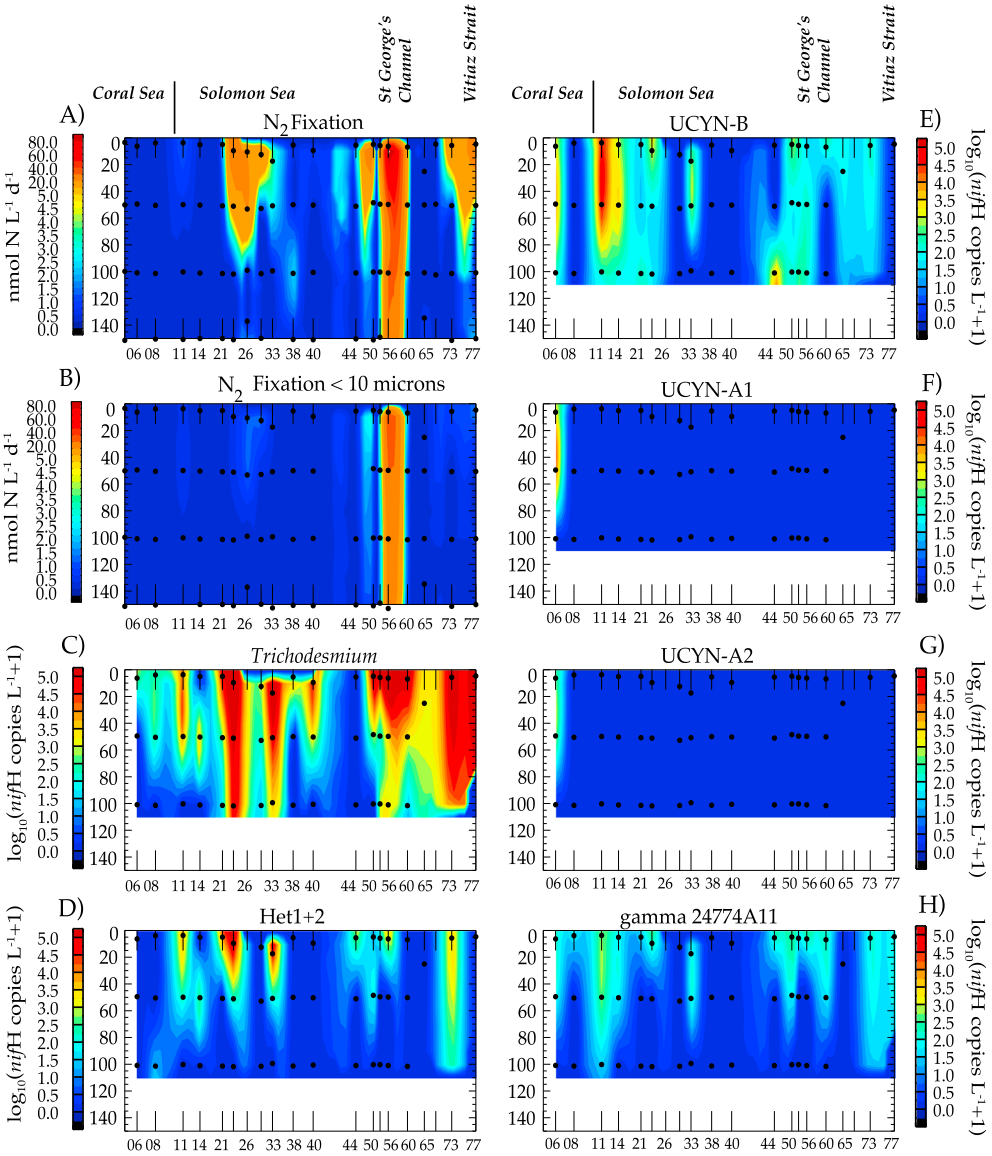

Figure 5. Horizontal and vertical distributions of N_2 fixation rates and diversity during the Pandora cruise (R/V *Atalante*). (a) Bulk N_2 fixation rates (nmol N L^{-1} d^{-1}), (b) N_2 fixation rates in fraction <10 μm (nmol N L^{-1} d^{-1}), (c) *Trichodesmium*, (d) Het-1 + Het-2, (e) UCYN-B, (f) UCYN-A1, (g) UCYN-A2, (h) γ-2474A11 abundances reported in log10 (*nif*H copies L^{-1} + 1). Station numbers are reported at the bottom of each panels.

3.4. Diazotroph Abundance and Distribution

Diazotroph abundances quantified using qPCR targeting the *nif*H gene reveal that the unicellular prymnesiophyte cyanobacterial symbiont UCYN-A was the most abundant diazotroph phylotype in the Coral Sea during the Bifurcation cruise (Figures 4f and 4g). The UCYN-A1 ecotype population dominated and was 120 times more abundant than the UCYN-A2 ecotype. UCYN-A1 abundances were highest at stations 39, 38, and 37 located close to New Caledonia, at the surface (5 m) or subsurface (40 m) ranging from 1 to 6×10^5 *nif*H copies L^{-1}. Their abundance decreased slightly at the northernmost stations but were still 2×10^4 *nif*H copies L^{-1} at station 11, where their maximum abundance was located deeper in the water column (75 m). UCYN-A2 and the heterotrophic diazotroph phylotype γ-24774A11 (Figures 4g and 4h) were the second most abundant *nif*H phylotypes during the Bifurcation cruise and followed the same distribution pattern as UCYN-A1, at abundances 1–2 orders of magnitude lower (ranging from $1–6 \times 10^3$ to $1–4 \times 10^2$ *nif*H copies L^{-1} for UCYN-A2 and γ-24774A11, respectively). UCYN-B was present only at station 37 at 70 m at low abundance

Table 1. Integrated (0–150 to 0–200 m) N_2 Fixation Rates (μmol N m^{-2} d^{-1}) Calculated From Measurements Performed During the Bifurcation and Pandora Cruises and Their Potential Contribution to New Primary Production

	Station	Areal rates (μmol m^{-2} d^{-1})	Contribution to NPP (%)
		Bifurcation cruise	
CORAL SEA	5	9	21
	10	4	35
	11	15	10
	15	65	36
	22	14	55
	27	22	6
	36	15	5
	37	24	19
	38	109	72
	39	87	36
	Average Bifurcation	*36*	*30*
	Average Coral Sea	*30*	*21*
		Pandora cruise	
SOLOMON SEA	3	16	5
	6	2	1
	8	4	0
	11	51	7
	14	9	2
	21	30	10
	23	786	90
	26	770	49
	29	296	80
	33	233	8
	38	132	ND
	40	28	2
	44	61	ND
	50	347	47
	53	36	ND
	56	5449	6264
	60	290	25
	65	10	1
	73	276	14
	77	612	49
	Average Pandora	*472*	*24 (391)*
	Average Solomon Sea	*624*	*34 (553)*

(10^2 *nif*H copies L^{-1}) (Figure 4e). *Trichodesmium* was present but at low abundances (10^2 to 10^3 *nif*H copies L^{-1}) in surface waters of stations 11 and 36 (Figure 4c). *Richelia* associated with *Rhizosolenia* and *Hemiaulus* (hereafter called Het-1 and Het-2, respectively) was observed only at 50 m at station 39 and in surface waters at station 36. UCYN-C were not detected in surface waters along the Bifurcation transect (data not shown).

During the Pandora cruise, UCYN-A, which were predominant during the Bifurcation cruise, were quasi-absent. UCYN-A1 and UCYN-A2 (Figures 5f and 5g) were detected only close to New Caledonia at station 6. However, *Trichodesmium* dominated the diazotroph community (Figure 5c) and was present throughout the transect from the surface to 100 m, with abundances increasing from the Coral Sea to the Solomon Sea. The highest abundances were measured in the St. George's Channel (station 56, 3.7×10^6 *nif*H copies L^{-1}), at the southern entrance of the Solomon Sea (station 23, 1.1×10^6 *nif*H copies L^{-1}) and in the Vitiaz Strait (station 77, 6.8×10^5 *nif*H copies L^{-1}). UCYN-B was the second most abundant diazotroph phylotype (Figure 5e) and reached maximum abundance of 6.3×10^4 *nif*H copies L^{-1} at station 11 at 50 m. γ-24774A11 (Figure 5h) followed the same distribution pattern as UCYN-B, but with lower abundances, particularly at depths greater than 50 m. Het-1 and Het-2 (Figure 5d) were present in the 0–50 m layer over a large part of the transect; as for *Trichodesmium*, maximum abundance ($2.3–3.8 \times 10^3$ *nif*H copies L^{-1}) was found in the St. George's Channel and in the Vitiaz Strait as well as at station 11 (5.8×10^3 *nif*H copies L^{-1}). UCYN-C were detected in surface of stations 11, 50, 60, and 73, but at abundances too low to be quantified (data not shown).

4. Discussion

This study provides some of the first data on N_2 fixation and diazotroph distributions in the Solomon Sea and the Coral Sea and should be a valuable contribution to the global diazotroph MAREDAT database [*Luo et al.*, 2012] for the SW Pacific and to the global biogeochemical N cycle. It reveals that N_2 fixation is an active process during austral winter conditions as it was detected at every single station. However, the magnitude of N_2 fixation rates and the diazotroph community composition in the two seas were quite different: integrated N_2 fixation rates over 0–150 m were an order of magnitude higher in the Solomon Sea compared

Table 2. Summary of Relationships Among Data Sets in the Coral Sea (Bifurcation Cruise) Indicated by Pearson Correlation Coefficients ($n = 20$)[a]

	Bulk N_2 Fixation	UCYN-A1 + A2	γ-24774A11	UCYN-B	*Trichodesmium*	Het-1 + Het-2	Temperature	Salinity	PO_4^{3-}	NO_x
Temperature	−0.46*	−0.54*	−0.51*	-	0.25	0.15	-	−0.95**	0.41	0.24
Salinity	0.56**	0.48*	0.40	-	−0.29	−0.17		-	−0.38	−0.15
PO_4^{3-}	−0.25	−0.26	−0.32	-	0	−0.04			-	0.24
NO_x	0.02	−0.19	−0.30	-	−0.11	−0.14				-
Primary prod	0.20	0.02	0.03	-	−0.01	0.20				
Chl *a*	−0.11	−0.37	−0.51*	-	−0.19	−0.13				
	Bulk N_2 fixation	N_2 fixation <10 μm	UCYN-A1 + A2	γ-24774A11	UCYN-B	*Trichodesmium*	Het-1 + Het-2			
Bulk N_2 fixation	-	0.99**	0.70**	0.50*	-	−0.05	−0.05			
N_2 fixation <10 μm		-	0.64**	0.48*	-	0	0			
UCYN-A1 + A2			-	0.79**	-	−0.11	−0.16			
γ-24774A11				-	-	0.31	0.22			
UCYN-B					-	-	-			
Trichodesmium						-	0.90**			
Het-1 + Het-2							-			

[a]All samples compared were from the 0 to 50 m upper layer.
*$p < 0.05$.
**$p < 0.01$.

to those measured in the Coral Sea during the same season. Moreover, while UCYN-A and γ-24774A11 dominated the diazotroph community in the Coral Sea and were both correlated with N_2 fixation rates ($p < 0.05$) (Table 2), *Trichodesmium* and UCYN-B dominated in the Solomon Sea and were correlated with N_2 fixation rates there ($p < 0.05$) (Table 3).

4.1. Influence of Environmental Conditions

During the Bifurcation cruise, the highest N_2 fixation rates were measured in the eastern part of the Coral Sea transect, close to New Caledonia, and were correlated with UCYN-A abundances ($p < 0.05$). Surface (0–50 m) UCYN-A abundances were inversely correlated ($p < 0.05$) with SST and correlated ($p < 0.05$) with salinity (Table 2). As nutrients were not correlated with temperature and salinity during the Bifurcation cruise (Table 2), these data suggest that UCYN-A were favored in this water mass characterized by low temperature (22.8–23.6°C) and high salinity (35.31–35.50), which are consistent with previous studies [*Agawin et al.*, 2014; *Moisander et al.*, 2010]. Such low-temperature/high-salinity conditions are typical of the region of the Coral Sea south of ~20°S and characteristic of surface water masses flowing from the west/southwest with the branches of the South Tropical Countercurrent [*Ceccarelli et al.*, 2013; *Kessler and Cravatte*, 2013; *Menkes et al.*, 2014; *Maes et al.*, 2013].

During the Pandora cruise, following a similar pattern, abundances of UCYN-A were inversely correlated with SST (Table 3) and their presence (although more sporadic than during the Bifurcation cruise) was restricted to the southernmost and coldest stations of the transect (Coral Sea) and was totally absent north of 15°S. This result provides further evidence that the UCYN-A/prymnesiophyte association had a preferential ecological niche in temperatures below 25°C and would explain why UCYN-A were abundant in Coral Sea and absent in the Solomon Sea. It has to be noted that both Bifurcation and Pandora cruises occurred during austral winter conditions, characterized by a 25°C isotherm located around 17°S compared to 26°S during summer conditions. This would mean that the UCYN-A would be restricted to more southern latitudes during the summer, which is consistent with the findings of *Moisander et al.* [2010].

Table 3. Summary of Relationships Among Data Sets in the Solomon Sea (Pandora Cruise) Indicated by Pearson Correlation Coefficients ($n = 38$)[a]

	Bulk N_2 Fixation	UCYN-A1 + A2	γ-24774A11	UCYN-B	*Trichodesmium*	Het-1 + Het-2	Temperature	Salinity	PO_4^{3-}	NO_x
Temperature	0.13	−0.50**	0.12	0.01	0.09	0.06	-	−0.11	0.11	−0.05
Salinity	−0.12	0.14	−0.45**	−0.36*	−0.14	−0.25	-	-	0.85**	0.63**
PO_4^{3-}	−0.19	-	−0.45**	−0.11	−0.23	−0.27	-	-	-	0.91**
NOx	−0.01	0.01	0.04	0.01	0.02	0.02	-	-	-	-
Primary production	0.34*	−0.15	−0.04	−0.15	0.35*	0.05	-	-	-	-
Chl *a*	0.33*	−0.08	−0.26	−0.25	0.29	−0.15	-	-	-	-
	Bulk N_2 fixation	N_2 fixation <10 μm	UCYN-A1 + A2	γ-24774A11	UCYN-B	*Trichodesmium*	Het-1 + Het-2			
Bulk N_2 fixation	-	0.91**	−0.08	0.16	−0.09	0.94**	0.27			
N_2 fixation <10 μm		-	−0.06	0.08	−0.07	0.74**	0.19			
UCYN-A1 + A2			-	−0.02	0.03	−0.06	−0.08			
γ-24774A11				-	0.79**	0.20	0.65**			
UCYN-B					-	−0.08	0.38*			
Trichodesmium						-	0.31			
Het-1 + Het-2							-			

[a]All samples compared were from the 0 to 50 m upper layer.
*$p < 0.05$.
**$p < 0.01$.

The γ-24774A11 abundances were correlated with UCYN-A during the Bifurcation cruise ($p < 0.01$; Table 2) and thus their abundances were also inversely correlated with SST. However, during the Pandora cruise, they were present throughout the transect and did not correlate with SST, indicating that they have a broader tolerance to SST when compared to UCYN-A. Despite being present at relatively low abundance ($1–4 \times 10^2$ *nif*H copies L^{-1}), they were the most ubiquitous diazotroph over the two cruises, supporting the hypothesized broad tolerance of this *nif*H phylotype to environmental parameters by *Moisander et al.* [2014] in the SW Pacific. UCYN-B and γ-24774A11 were inversely correlated with salinity during the Pandora cruise ($p < 0.05$; Table 3) and totally absent at low-salinity stations 8, 38, and 40. *Moisander et al.* [2010] also reported an inverse correlation between UCYN-B abundances and salinity. The role of salinity in the physiology of these diazotrophs is not well understood and would need further investigations.

As optimal growth rate and nitrogenase activity of *Trichodesmium* are reached at high temperatures (24–30°C) [*Breitbarth et al.*, 2007], one can hypothesize that the higher SST in the Solomon Sea (25.3–29.6°C) compared to the Coral Sea (22.8–26.2°C) at the time of the cruises likely explains the higher *Trichodesmium* abundances and the higher N_2 fixation rates in the Solomon Sea. However, N_2 fixation and *Trichodesmium* abundances were weakly correlated with temperature ($p > 0.1$), both when considering data from only the Solomon Sea and when considering data from the two cruises together. Moreover, *Trichodesmium* was absent or present at very low abundances in the Coral Sea ($0–5 \times 10^2$ *nif*H copies L^{-1}) even at stations located above the 24°C isotherm, indicating that temperature alone cannot explain the differences in observed distributions between the two cruises. *Shiozaki et al.* [2014] describe an island mass effect mechanism in the SW Pacific in which active N_2 fixation and high *Trichodesmium* abundances are observed near islands (New Caledonia, Vanuatu, and Fiji) due to nutrients supplied by land runoff that fuel high primary production around the archipelagos. We hypothesize that the same phenomenon occurs in the Solomon Sea, which is surrounded by many islands (Figure 1a),

maintaining high PO_4^{3-} concentrations (always >0.08 μmol L^{-1}), which, together with SST > 25°C, would favor high abundances of *Trichodesmium* in the Solomon Sea. The lack of relationship between *Trichodesmium* abundances and nutrient distributions, especially PO_4^{3-} (Table 3), is not contrary to this hypothesis since the diazotrophs can both be impacted by the PO_4^{3-} and have an impact on PO_4^{3-} via assimilation. *Trichodesmium* is also known to synthesize hydrolytic enzymes in order to access the dissolved organic phosphorus pool (DOP) [*Sohm and Capone*, 2006]. We cannot exclude that DOP played a role in maintaining high *Trichodesmium* biomass in the Solomon Sea, although DOP uptake often occurs when inorganic PO_4^{3-} is in short supply, which was not the case in this study, since PO_4^{3-} concentrations were always greater than cellular P requirements for both *Trichodesmium* [*Moutin et al.*, 2005] and the <10 μm diazotroph community [*Falcón et al.*, 2005; *Lin et al.*, 2011].

In addition to PO_4^{3-}, the supply mechanisms of the micronutrient Fe, which is a major component of the nitrogenase enzyme that catalyzes N_2 fixation [*Raven*, 1988], may contribute to explain the differences observed in N_2 fixation between the Coral and the Solomon Sea. As pointed above, the Solomon Sea is a semi-enclosed basin surrounded by many islands. According to Fe isotopic data, it receives continuous Fe sources from land runoff, hydrothermal, and volcanic activity [*Labatut et al.*, 2014]. The dFe measurements performed along a west-east zonal section in the equatorial Pacific [*Slemons et al.*, 2010] confirmed that the north of the Solomon Sea was a primary source of dFe for the equatorial Pacific. On the opposite, the Coral Sea is a remote area and the major Fe inputs are likely associated with atmospheric deposition, which are quite low (0.2−0.5 g m^{-2} yr^{-1}) compared to the Atlantic or the Mediterranean Sea (2–50 g m^{-2} yr^{-1}) [*Jickells et al.*, 2005]. The dFe measurements performed at some selected stations during the Pandora cruise (Figure 1a) [*Quéroué and Sarthou*, unpublished data] confirm that concentrations in the euphotic zone (~0–150 m, i.e. where most of the diazotrophs detected in this study are able to grow) were significantly ($p < 0.05$) higher at stations located near the coast in the Solomon Sea (0.35 ± 0.06 nmol L^{-1}) compared to stations located in the Coral Sea (0.23 ± 0.07 nmol L^{-1}). At offshore stations in the Solomon Sea, the dFe concentrations of 0.19 ± 0.02 nmol L^{-1} were not significantly different ($p > 0.05$) from those measured in the Coral Sea. However, dFe stocks have to be considered with caution as they are the results of Fe inputs minus outputs (biological consumption, adsorption onto particles). Although Fe inputs might be higher in the Solomon Sea than in the Coral Sea, the high primary production and *Trichodesmium* abundance may have contributed to consume dFe, which likely explains the low difference of dFe stocks between the Coral and the Solomon Seas. Fe dynamics alone cannot explain the diazotroph distribution observed in the studied area; however, the literature and the above-mentioned data would indicate that the Coral Sea may have been more Fe limited at the time of this study than the Solomon Sea. This is in accordance with *Moisander et al.* [2011], who reported that UCYN-A abundances increased in response to Fe additions in the Coral Sea. *Trichodesmium* has higher cellular Fe requirements than those of UCYN [*Berman-Frank et al.*, 2001] and likely fix N_2 at higher cell specific rates than some UCYN phylotypes (e.g., *Crocosphaera* [*Foster et al.*, 2013; *Capone et al.*, 1997]), which may explain the dominance of *Trichodesmium* as well as the higher N_2 fixation rates in the Solomon Sea compared to the Coral Sea.

During both cruises, the highest N_2 fixation rates were measured in surface (0–50 m) waters, where NO_x concentrations were close to DL, which is a classical pattern given the high energetic cost necessary to break the triple bound of the N_2 molecule compared to the assimilation of NO_3 [*Falkowski*, 1983]. However, rates as high as ~20 nmol N L^{-1} d^{-1} were measured at 100 and 150 m depths at station 56 during the Pandora cruise, where NO_x concentrations were ~5 μmol L^{-1}. This is also the case during Bifurcation, where rates of ~1 nmol N L^{-1} d^{-1} were measured at 50 m depth at station 15, where NO_x concentrations were ~1 μmol L^{-1}. These surprisingly high rates are unlikely due to contaminations of the $^{15}N_2$ stocks used in this study (Cambridge Isotopes) as they contained low concentrations of ^{15}N contaminants, and the potential overestimation of N_2 fixation rates are <0.02 nmol N L^{-1} d^{-1}. Significant N_2 fixation rates have already been reported in culture [*Dekaezemacker and Bonnet*, 2011; *Knapp et al.*, 2012; *Holl and Montoya*, 2005] and in the field [*Dekaezemacker et al.*, 2013; *Raimbaut and Garcia*, 2008] in the presence of high (2–30 μM) NO_3^- concentrations, but these field rates were an order of magnitude lower than those reported during the Pandora cruise. The underlying physiological mechanisms involved in PNG deep waters remain to be studied, as well as the organisms responsible for these high rates. They did not match with any of the qPCR assays tested in this study but are likely organisms <10 μm, since 70% of the rates were measured in the <10 μm fraction at 100 and 150 m.

4.2. Hydrodynamics and *Trichodesmium* Distribution

Due to the buoyancy of *Trichodesmium*, its distribution may also depend on the hydrodynamics of surface or near-surface waters [*Capone et al.*, 1997].

Trichodesmium were most abundant in the Pandora cruise at the northern exit of the Solomon Sea in the St. George's Channel (station 56, 3.8×10^6 *nif*H copies L^{-1}), in the Vitiaz Strait (station 77, 6.8×10^5 *nif*H copies L^{-1}), and at the southern entrance of the Solomon Sea (station 23, 1.1×10^6 *nif*H copies L^{-1}) (Figure 5c). The associated N_2 fixation rates were extremely high at these locations (up to 5187 μmol N m^{-2} d^{-1}), i.e., among the highest rates reported in the literature, which is in accordance with the extremely high rates measured in the Vitiaz Strait in 2006 (11 900 μmol N m^{-2} d^{-1}) [*Bonnet et al.*, 2009]. St. George's Channel (30 km wide) and Vitiaz Strait (45 km wide) are two narrow passages for waters exiting the Solomon Sea toward the equator. They are characterized by very strong currents, turbulence, and high convergence [*Djath et al.*, 2014; *Cravatte et al.*, 2011], which was confirmed during the Pandora cruise (Figure 2). Horizontal advection has been evoked as a recurrent hypothesis for the surface accumulation of positively buoyant material such as *Trichodesmium* [*Dandonneau et al.*, 2003]. The high *Trichodesmium* abundances and high associated N_2 fixation rates measured in these two straits indicate that they both act as bottlenecks for the surface waters, thus consistent with this hypothesis.

The surface currents measured by ADCP (Figure 2) show a strong near-surface northward current toward the Bismarck Sea through the Vitiaz Strait and the St. George's Channel. This indicates that the buoyant *Trichodesmium* accumulated in the straits and channels at the north of Solomon Sea are probably transported from their initial production zone, which may affect N inventories and primary productivity farther north in the equatorial Pacific. This highlights the necessity to reinforce coupled physical-biogeochemical studies if we want to better understand the distribution and biogeochemical impact of N_2 fixation in the ocean.

When considering instantaneous measurements, the circulation in the Solomon Sea is largely dominated by mesoscale and submesoscale features [*Gourdeau et al.*, 2014] and small submesoscale frontal structures may locally concentrate *Trichodesmium* as reported in the tropical Atlantic [*Davis and McGillicuddy*, 2006; *Olson et al.*, 2015] and Pacific oceans [*Fong et al.*, 2008; *Church et al.*, 2009]. Figure 6 shows the local salinity at high resolution along the cruise track which, in the presence of a background, smooth salinity gradient, would be the signature of a local convergence in the surface current [*Maes et al.*, 2013]. However, no significant correlation ($p < 0.05$) between salinity gradient and *Trichodesmium nif*H copies L^{-1} was found, possibly because the salinity gradient is a weak marker of surface water convergence as it is conditioned by the presence of a background salinity gradient. Future work using front detection via FSLE (Finite Size Lyapunov Exponents [e.g., *d'Ovidio et al.*, 2009]), may be able to show the correlation between *Trichodesmium* accumulation and density fronts. However, the use of FSLE based on altimetric data is limited here due to the complex bathymetry and the presence of numerous islands and narrow straits.

4.3. Diazotroph Abundance and Distributions

In the Coral Sea, the correlation between N_2 fixation rates and UCYN-A (UCYN-A1 and UCYN-A2) and γ-24774A11 abundances (Bifurcation cruise; Table 2) is consistent with the fact that N_2 fixation associated with the <10 μm size fraction accounted for 70% of total N_2 fixation. Thus, the UCYN-A/prymnesiophyte associations were likely the major contributors to N_2 fixation in the Coral Sea as their abundances were strongly correlated with both the bulk and <10 μm N_2 fixation rates ($p<0.01$; Table 2). The measured abundances of UCYN-A, which ranged from 1 to 6×10^5 *nif*H copies L^{-1}, were in the upper range of abundances reported in the global MAREDAT database [*Luo et al.*, 2012] and of the same order of magnitude of those reported at station ALOHA in the North Pacific subtropical gyre [*Church et al.*, 2005a]. However, *Moisander et al.* [2010] reported abundance as much as an order of magnitude higher (up to 6×10^6 *nif*H copies L^{-1}) in the Coral Sea during the austral summer, suggesting a possible seasonal effect on the growth of UCYN-A/prymnesiophyte association that can only be resolved with higher spatial/temporal resolution data. Both subclades of the UCYN-A/prymnesiophyte association (UCYN-A1 and UCYN-A2) were present in the Coral Sea and were strongly correlated ($p < 0.01$) with each other; however, UCYN-A1 was on average 120 times more abundant than UCYN-A2 over the cruise. The UCYN-A2 subclade was always associated with the presence of UCYN-A1 but not vice versa. It has been demonstrated that UCYN-A1 and UCYN-A2 each associate

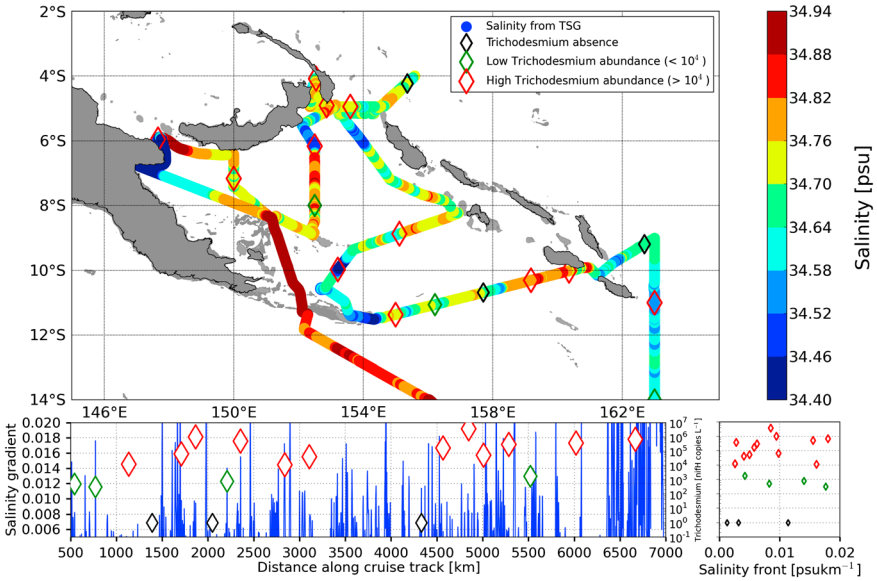

Figure 6. Salinity fronts detection and surface (0–30 m) *Trichodesmium* distributions. (top) Pandora cruise track with salinity from the thermosalinograph. Colored diamonds indicate different *Trichodesmium* abundance as indicated in the legend ("high abundance" is $>10^4$ *nif*H copies L^{-1}; "low abundance" is $<10^4$ *nif*H copies L^{-1}). (bottom left) Blue: salinity gradient (psu km^{-1}) along the cruise track and diamonds: *Trichodesmium* abundance (*nif*H copies L^{-1}) as indicated in Figure 6 (top) legend for the 0–30 m upper layer. (bottom right) Same as Figure 6 (bottom left) but as *Trichodesmium* abundances versus salinity gradients.

with different strains of *Braarudosphaera bigelowii*, and there is some indication that each host symbiont pair may have adapted to a specific environmental niche, with the UCYN-A2/prymnesiophyte association more commonly found at high abundances in coastal regions [*Thompson et al.*, 2014, 2012]. This is the first report of the UCYN-A2/prymnesiophyte association in the SW Pacific, and it appears to be restricted to the cold and salty surface water mass of the South Tropical Countercurrent branches close to New Caledonia, which provides additional evidence that it may favor coastal niches. In contrast, the UCYN-A1/prymnesiophyte association was more abundant and widely distributed, and its population extended deeper in the water column, indicating a probable broader tolerance of the UCYN-A1/prymnesiophyte association to environmental parameters.

In addition to the UCYN-A/prymnesiophyte associations, ɤ-24774A11 may have also contributed to N_2 fixation in the Coral Sea as their abundance were correlated with both bulk and $<10\,\mu m$ N_2 fixation rates ($p < 0.05$; Table 2), but the correlation was weaker than for UCYN-A. The ɤ-24774A11 is one of the most commonly reported marine heterotrophic diazotroph and has been quantified in several coastal and open ocean areas such as the North Pacific [*Church et al.*, 2005b], South Pacific [*Moisander et al.*, 2014], North Atlantic [*Langlois et al.*, 2005], and Red Sea [*Foster et al.*, 2009] and has been observed actively transcribing *nif*H as well [*Moisander et al.*, 2014; *Zehr et al.*, 2007], but active N_2 fixation of this uncultivated phylotype has yet to be proven [*Turk-Kubo et al.*, 2013]. Non-cyanobacterial diazotrophs are not restricted to the photic zone, like their cyanobacterial counterparts, and have been detected in mesopelagic waters [*Fernandez et al.*, 2011; *Bonnet et al.*, 2013; *Hamersley et al.*, 2011; *Hewson et al.*, 2007; *Turk-Kubo et al.*, 2013] and are hypothesized to contribute to in situ N_2 fixation activity in areas where depth-integrated rates can exceed those measured in the photic zone as in the eastern South Pacific [*Bonnet et al.*, 2013]. *Moisander et al.* [2014] recently concluded that they should be considered carefully as potential global contributors of N_2 fixation in the SW Pacific due to their consistent *nif*H expression over large geographical distances. The ɤ-24774A11 abundances were correlated with the abundance of UCYN-A in the Coral Sea ($p < 0.05$; Table 2) and UCYN-B and Het-1 + Het-2 in the Solomon Sea ($p < 0.05$; Table 3). Moreover, they were rarely observed alone in the photic zone but always associated with other cyanobacterial diazotrophs, i.e. UCYN-A1 in the Coral Sea and with UCYN-B in the Solomon Sea (except at three data points over the 50 studied). Further studies are needed to study the potential link between ɤ-24774A11 and other *nif*H phylotypes in the ocean.

Two notable results of this study are the absence of UCYN-A in the Solomon Sea despite being considered the most abundant and most widespread cyanobacterial diazotroph in the world [*Luo et al.*, 2012], as well as the quasi-absence of UCYN-B and *Trichodesmium* in the Coral Sea, at least in austral winter. During the Pandora cruise, UCYN-A were present only at the two coldest stations (stations 3 and 6) located at the eastern border of the Coral Sea and disappeared north of 15°S, where *Trichodesmium* and UCYN-B abundances started to increase. *Moisander et al.* [2010] reported a transition zone from *Crocosphaera* (UCYN-B)-dominated communities in warm surface waters to UCYN-A-dominated communities in cooler waters of the SW Pacific, which is in agreement with our results. In their study, abundance of *Trichodesmium* and UCYN-B was correlated, and both of them were inversely correlated with UCYN-A abundances. In contrast, *Campbell et al.* [2005] report an inverse correlation between *Trichodesmium* and *Crocosphaera*-like (UCYN-B) distributions between New Caledonia and Fiji. In our study, we could not see any significant positive or inverse correlation between *Trichodesmium*, UCYN-B, and UCYN-A over the two cruises. These conflicting results for three cruises performed in the SW Pacific indicate that the biogeographical distribution of diazotrophs is likely very complex. However, some common patterns emerge. First, there is a separation of ecological niches between the UCYN-A/prymnesiophyte associations and other cyanobacterial diazotrophs. It is extremely pronounced in our study as UCYN-A were absent when UCYN-B and *Trichodesmium* were present (Solomon Sea) and, inversely, UCYN-B and *Trichodesmium* were absent or quasi absent when UCYN-A were present (Coral Sea). Second, temperature is consistently ([*Moisander et al.*, 2010], this study) the most significant factor inversely correlated with the abundance of the UCYN-A/prymnesiophyte associations.

In the Solomon Sea, the strong correlation ($p < 0.01$) between N_2 fixation rates and *Trichodesmium* abundances is consistent with the fact that only 35% of N_2 fixation rates were measured in the $<10\,\mu m$ size fraction. *Trichodesmium* were likely the major contributors to N_2 fixation as well as *Richelia intracellularis* in association with *Rhizosolenia* spp. (Het-1) and *Hemiaulus* spp. (Het-2). Although Het-1 and Het-2 abundances have been summed for the purpose of this study, Het-1 were more abundant and widely distributed compared to Het-2 (data not shown). In their synthesis, *Foster and O'Mullan* [2008] report higher abundances of Het-2 in the Atlantic Ocean [e.g., *Foster et al.*, 2007; *Villareal*, 1991] and Het-1 in the North Pacific central gyre [e.g., *Mague et al.*, 1974], which is in agreement with our observations. Moisander et al. (Unpublished, reported in the MAREDAT [*Luo et al.*, 2012] database) reported similar orders of magnitude of Het-1 and Het-2 abundances in the SW Pacific as those reported here (10^2–10^3 *nif*H copies L^{-1}). In the Coral Sea, Het-1 and Het-2 abundances were correlated with *Trichodesmium* abundances despite both groups being rarely detected or present at low abundances (10^2 *nif*H copies L^{-1}). In the Solomon Sea, abundances were higher (10^3 *nif*H copies L^{-1}) and not correlated with *Trichodesmium* abundances, which is a result contrary to *Moisander et al.* [2010], and they were correlated with UCYN-B and γ-24774A11 abundances. However, their abundances did not correlate with any of the environmental parameters measured during the cruise (Table 3), suggesting that other factors may control their spatial distribution.

Finally, *Crocosphaera* (UCYN-B) were often microscopically observed in the $>10\,\mu m$ fraction during the Pandora cruise; therefore, we cannot exclude its contribution to N_2 fixation in the $>10\,\mu m$ size fraction. Despite their nanoplanktonic size, *Crocosphaera*-like cells have also been reported in the $>10\,\mu m$ size fraction by *Bonnet et al.* [2009] in the equatorial Pacific, probably due to the formation of large ($>10\,\mu m$) sticky aggregates resulting from the production of sizable amounts of exopolysaccharides [*Sohm et al.*, 2011b]. In the present study, they were observed as aggregates in the $>10\,\mu m$ and associated with the diatom *Climacodium* (data not shown).

4.4. Potential Biogeochemical Impact of N_2 Fixation in the Coral and Solomon Seas

N_2 fixation rates measured within the Solomon Sea ranged from 30 to 5449 $\mu mol\,N\,m^{-2}\,d^{-1}$ (average 624 $\pm$ 1360 $\mu mol\,N\,m^{-2}\,d^{-1}$; Table 1) and are in the upper range (100–1000 $\mu mol\,m^{-2}\,d^{-1}$) of the rates compiled in the global N_2 fixation MAREDAT database [*Luo et al.*, 2012]. N_2 fixation rates surpassed this upper range at station 56. This indicates that the Solomon Sea is one of the highest N_2 fixation areas in the global ocean. Assuming that diazotrophs fix on average 624 $\mu mol\,m^{-2}\,d^{-1}$ throughout the year and considering a Solomon Sea area of $7.2 \times 10^{11}\,m^2$, N_2 fixation in this area would introduce 2.5 Tg N yr^{-1}. This corresponds to 10% of the total N fixed for the entire South Pacific Ocean reported by [*Luo et al.*, 2012], while the Solomon Sea represents only 1% of its total area. Consequently, the N_2 fixation budget for the South Pacific probably needs to be revised by including the recent studies performed in the SW Pacific [i.e., *Shiozaki et al.*, 2014, this study].

In the Solomon Sea, N_2 fixation was correlated with primary production ($p < 0.05$), indicating that primary production was potentially supported by N_2 fixation. Based on a C:N ratio of 7 and ^{13}C data (not shown), N_2 fixation accounted on average for 31% of the N demand of total primary productivity in the Solomon Sea and 5.5% if the extremely high N_2 fixation value at station 56 is excluded. As N_2 fixation represents a source of new N (as opposed to recycled N), it is more appropriate to compare N_2 fixation rates with new production, which has been derived from primary production according to the following equation determined by *Raimbault and Garcia* [2008] in the tropical south Pacific:

$$\text{New production} = 0.017(\text{Primary production})^{1.6965}$$

N_2 fixation, on average, accounted for 34% of the N demand in the Solomon Sea (Table 1) if we exclude station 56 and 100% if we include it. This indicates that N_2 fixation was of major biogeochemical importance in the Solomon Sea at that time of the year. No other data exist from the Solomon Sea for comparison, but *Shiozaki et al.* [2010] and *Bonnet et al.* [2009] report that new primary production was also mainly supported by N_2 fixation in the warm pool north of the Solomon Sea, indicating that the high N_2 fixation hot spot is probably not limited to the Solomon Sea and may extends northward.

In the Coral Sea, N_2 fixation rates ranged from 2 to 109 $\mu mol\ N\ m^{-2}\ d^{-1}$ (average $30 \pm 33\ \mu mol\ N\ m^{-2}\ d^{-1}$; Table 1) during the austral winter and are in the lowest range (1–100 $\mu mol\ N\ m^{-2}\ d^{-1}$) of rates reported by *Luo et al.* [2012] in the global database. Unlike the Solomon Sea, N_2 fixation was not significantly ($p > 0.05$) correlated with primary productivity. The contribution of N_2 fixation to new primary production was on average 21%, indicating that other sources of N probably sustained the major part of primary production in this area.

5. Conclusions

This study presents the distribution of N_2 fixation and *nif*H phylotypes in the Coral and Solomon Seas during austral winter conditions. N_2 fixation activity displays a large regional variability with a "hot spot" in the previously unreported Solomon Sea, likely due to high *Trichodesmium* abundance, which have been attributed to SST > 25°C associated with high PO_4^{3-} and possibly Fe supply provided by land runoff and volcanic inputs. In contrast, the Coral Sea exhibited N_2 fixation rates 20 times lower on average and was dominated by UCYN-A, which was attributed to a preferential ecological niche of this association for SST < 25°C. Further studies need to be done during austral summer conditions to evaluate the diversity and biogeochemical role of diazotrophs during the most favorable season for N_2 fixation.

Acknowledgments
These projects are co-funded by ANR (project ANR-09-BLAN-0233-01), INSU/LEFE (IMAGO and CYBER), IRD, and LEGOS. The Pandora cruise is a contribution to the CLIVAR/SPICE and GEOTRACES International programs. We thank the captains and crew of the R/V *Alis* and *Atalante*. We also thank F. Baurand, Philippe Gérard, and the LAMA (US IMAGO IRD) for nutrients analyses. K.T.K. is supported through the Gordon and Betty Moore Foundation's Marine Microbial Initiative awarded to Jonathan Zehr (UCSC). Data presented in this article are available in the LEFE-CYBER database http://www.obs-vlfr.fr/proof/php/pandora/x_datalist_1.php?xxop=pandora&xxcamp=pandora.

References

Agawin, N. S. R., M. Benavides, A. Busquets, P. Ferriol, L. Stal, and J. Aristegui (2014), Dominance of unicellular cyanobacteria in the diazotrophic community in the Atlantic Ocean, *Limnol. Oceanogr.*, *59*, 627–637.

Aminot, A., and R. Kerouel (2007), *Dosage Automatique des Nutriments Dans les Eaux Marines*, p. 188, Editions de l'Ifremer, Paris.

Berman-Frank, I., J. J. Cullen, Y. Hareli, R. Sherrell, and P. G. Falkowski (2001), Iron availability, cellular iron quotas, and nitrogen fixation in *Trichodesmium*, *Limnol. Oceanogr.*, *46*, 1249–1277.

Bonnet, S., et al. (2008), Nutrient limitation of primary productivity in the Southeast Pacific (BIOSOPE cruise), *Biogeosciences*, *5*, 215–225.

Bonnet, S., I. C. Biegala, P. Dutrieux, L. O. Slemons, and D. G. Capone (2009), Nitrogen fixation in the western equatorial Pacific: Rates, diazotrophic cyanobacterial size class distribution, and biogeochemical significance, *Global Biogeochem. Cycles*, *23*, GB3012, doi:10.1029/2008GB003439.

Bonnet, S., O. Grosso, and T. Moutin (2011), Planktonic dinitrogen fixation along a longitudinal gradient across the Mediterranean Sea during the stratified period (BOUM cruise), *Biogeosciences*, *8*, 2257–2267.

Bonnet, S., J. Dekaezemacker, K. A. Turk-Kubo, T. Moutin, R. M. Hamersley, O. Grosso, J. P. Zehr, and D. G. Capone (2013), Aphotic N_2 fixation in the eastern tropical South Pacific Ocean, *PLoS One*, *8*(12), e81265, doi:10.1371/journal.pone.0081265.

Breitbarth, E., A. Oschlies, and J. LaRoche (2007), Physiological constraints on the global distribution of *Trichodesmium* - effect of temperature on diazotrophy, *Biogeosciences*, *4*(1), 53–61.

Buitenhuis, E. T., et al. (2012), Picophytoplankton biomass distribution in the global ocean, *Earth Syst. Sci. Data*, doi:10.5194/essd-5194-5137-2012.

Campbell, L., E. J. Carpenter, J. P. Montoya, A. B. Kustka, and D. G. Capone (2005), Picoplankton community structure within and outside a *Trichodesmium* bloom in the southwestern Pacific Ocean, *Vie et Milieu-Life and Environ.*, *55*, 185–195.

Capone, D. G., J. P. Zehr, H. W. Paerl, B. Bergman, and E. J. Carpenter (1997), *Trichodesmium*, a globally significant marine cyanobacterium, *Science*, *276*, 1221–1229.

Ceccarelli, D. M., et al. (2013), The coral sea: Physical environment, ecosystem status and biodiversity assets, *Adv. Mar. Biol.*, *66*, 213–290.

Church, M. J., B. D. Jenkins, D. M. Karl, and J. P. Zehr (2005a), Vertical distributions of nitrogen-fixing phylotypes at Stn ALOHA in the oligotrophic North Pacific Ocean, *Aquat. Microb. Ecol.*, *38*(1), 3–14.

Church, M. J., C. M. Short, B. D. Jenkins, D. M. Karl, and J. P. Zehr (2005b), Temporal patterns of nitrogenase gene (*nif*H) expression in the oligotrophic North Pacific Ocean, *Appl. Environ. Microbiol.*, *71*(9), 5362–5370.

Church, M. J., C. Mahaffey, R. M. Letelier, R. Lukas, J. P. Zehr, and D. M. Karl (2009), Physical forcing of nitrogen fixation and diazotroph community structure in the North Pacific subtropical gyre, *Global Biogeochem. Cycles*, *23*, GB2020, doi:10.1029/2008GB003418.

Codispoti, L. A., J. A. Brandes, J. P. Christensen, A. H. Devol, S. W. A. Naqvi, H. W. Paerl, and T. Yoshinari (2001), The oceanic fixed nitrogen and nitrous oxide budgets: Moving targets as we enter the anthropocene?, *Sci. Mar.*, *65*(S2), 85–105.

Cravatte, S., A. Ganachaud, Q. P. Duong, W. S. Kessler, G. Eldin, and P. Dutrieux (2011), Observed circulation in the Solomon Sea from SADCP data, *Prog. Oceanogr.*, *88*(1–4), 116–130.

Dabundo, R., M. F. Lehmann, L. Treibergs, C. R. Tobias, M. A. Altabet, A. M. Moisander, and J. Granger (2014), The contamination of commercial $^{15}N_2$ gas stocks with ^{15}N–Labeled nitrate and ammonium and consequences for nitrogen fixation measurements, *PLoS One*, *9*(10), e110335, doi:10.1371/journal.pone.0110335.

Dandonneau, Y., A. Vega, H. Loisel, Y. du Penhoat, and C. Menkes (2003), Oceanic Rossby waves acting as a "hay rake" for ecosystem floating by-products, *Science*, *302*(5650), 1548–1551.

Davis, C. S., and D. J. McGillicuddy (2006), Transatlantic abundance of the N_2-fixing colonial cyanobacterium *Trichodesmium*, *Science*, *312*, 1517–1519.

Dekaezemacker, J., and S. Bonnet (2011), Sensitivity of N_2 fixation to combined nitrogen forms (NO_3^- and NH_4^+) in two strains of the marine diazotroph *Crocosphaera watsonii* (Cyanobacteria), *Mar. Ecol. Prog. Ser.*, *438*, 33–46.

Dekaezemacker, J., S. Bonnet, O. Grosso, T. Moutin, M. Bressac, and D. Capone (2013), Evidence of active dinitrogen fixation in surface waters of the eastern tropical south Pacific during El Nino and La Nina events and evaluation of its potential nutrient controls, *Global Biogeochem. Cycles*, *27*, 768–779, doi:10.1002/gbc.20063.

Deutsch, C., J. L. Sarmiento, D. M. Sigman, N. Gruber, and J. P. Dunne (2007), Spatial coupling of nitrogen inputs and losses in the ocean, *Nature*, *445*, 163–167.

Djath, B., J. Verron, L. Gourdeau, A. Melet, B. Barnier, and J. M. Molines (2014), Multiscale analysis of dynamics from high resolution realistic model of the solomon sea, *J. Geophys. Res. Oceans*, *119*, 6286–6304, doi:10.1002/2013JC009695.

d'Ovidio, F., J. Isern-Fontanet, C. López, E. García-Ladona, and E. Hernández-García (2009), Comparison between Eulerian diagnostics and the finite-size Lyapunov exponent computed from altimetry in the Algerian Basin, *Deep Sea Res., Part I*, *56*, 15–31.

Eldin, G., A. Ganachaud, S. Cravatte, and C. Jeandel (2013), Pandora cruise provides an unprecedented description of the Solomon Sea, *CLIVAR Newsl. Exch.*, *61*(18), 24–25.

Falcón, L., S. Pluvinage, and E. J. Carpenter (2005), Growth kinetics of marine unicellular N_2-fixing cyanobacterial isolates in continuous culture in relation to phosphorus and temperature, *Mar. Ecol. Prog. Ser.*, *28*, 3–8.

Falkowski, P. G. (1983), Light-shade adaptation and vertical mixing of marine phytoplankton: A comparative field study, *J. Mar. Res.*, *41*, 215–237.

Fernandez, C., L. Farías, and O. Ulloa (2011), Nitrogen fixation in denitrified marine waters, *PLoS One*, *6*(6), e20539, doi:10.1371/journal.pone.0020539.

Fong, A. A., D. M. Karl, R. Lukas, R. M. Letelier, J. P. Zehr, and M. J. Church (2008), Nitrogen fixation in an anticyclonic eddy in the oligotrophic North Pacific Ocean, *ISME J.*, *2*(6), 663–676.

Foster, R., and G. D. O'Mullan (2008), *Nitrogen-Fixing and Nitrifying Symbioses in the Marine Environment*, Academic Press, London.

Foster, R., A. Paytan, and J. P. Zehr (2009), Seasonality of N_2 fixation and *nif*H diversity in the Gulf of Aqaba, *Limnol. Oceanogr.*, *54*, 219–233.

Foster, R. A., A. Subramaniam, C. Mahaffey, E. J. Carpenter, D. G. Capone, and J. P. Zehr (2007), Influence of the Amazon River plume on distributions of free-living and symbiotic cyanobacteria in the western tropical north Atlantic Ocean, *Limnol. Oceanogr.*, *52*(2), 517–532.

Foster, R. A., S. Sztejrenszus, and M. M. M. Kuypers (2013), Measuring carbon and N_2 fixation in field populations of colonial and free living cyanobacteria using nanometer scale secondary ion mass spectrometry, *J. Phycol.*, *49*, 502–516.

Ganachaud, A., et al. (2014), The Southwest Pacific Ocean and Climate Experiment (SPICE), *J. Geophys. Res. Oceans*, *119*, 7660–7686, doi:10.1002/2013JC009678.

Garcia, N., P. Raimbault, and V. Sandroni (2007), Seasonal nitrogen fixation and primary production in the Southwest Pacific: Nanoplankton diazotrophy and transfer of nitrogen to picoplankton organisms, *Mar. Ecol. Prog. Ser.*, *343*, 25–33.

Goebel, N. L., K. A. Turk, K. M. Achilles, R. Paerl, I. Hewson, A. E. Morrison, J. P. Montoya, C. A. Edwards, and J. P. Zehr (2010), Abundance and distribution of major groups of diazotrophic cyanobacteria and their potential contribution to N_2 fixation in the tropical Atlantic Ocean, *Environ. Microbiol.*, *12*(12), 3272–3789.

Gourdeau, L., J. Verron, A. Melet, W. Kessler, F. Marin, and B. Djath (2014), Exploring the mesoscale activity in the Solomon Sea: A complementary approach with a numerical model and altimetric data, *J. Geophys. Res. Oceans*, *119*, 2290–2311, doi:10.1002/2013JC009614.

Gruber, N. (2004), The dynamics of the marine nitrogen cycle and its influence on atmospheric CO_2, in *The Ocean Carbon Cycle and Climate*, edited by M. Follows and T. Oguz, pp. 97–51, Kluwer Acad., Dordrecht.

Halm, H., P. Lam, T. G. Ferdelman, G. Lavik, T. Dittmar, J. LaRoche, S. D'Hondt, and M. M. M. Kuypers (2012), Heterotrophic organisms dominate nitrogen fixation in the South Pacific Gyre, *ISME J.*, *6*(6), 1238–1249.

Hamersley, M. R., K. A. Turk, A. Leinweber, N. Gruber, J. P. Zehr, T. Gunderson, and D. G. Capone (2011), Nitrogen fixation within the water column associated with two hypoxic basins in the Southern California Bight, *Aquat. Microb. Ecol.*, *63*(2), 193–205.

Herbland, A., A. Lebouteiller, and P. Raimbault (1985), Size structure of phytoplankton biomass in the equatorial Atlantic Ocean, *Deep Sea Res.*, *32*, 819–836.

Hewson, I., P. H. Moisander, K. M. Achilles, C. A. Carlson, B. D. Jenkins, E. A. Mondragon, A. E. Morrison, and J. P. Zehr (2007), Characteristics of diazotrophs in surface to abyssopelagic waters of the Sargasso Sea, *Aquat. Microb. Ecol.*, *46*(1), 15–30.

Holl, C. M., and J. P. Montoya (2005), Interactions between nitrate uptake and nitrogen fixation in continuous cultures of the marine diazotroph *Trichodesmium* (Cyanobacteria), *J. Phycol.*, *41*(6), 1178–1183.

Hristova, H., W. S. Kessler, J. C. McWilliams, and M. J. Molemaker (2014), Eddy distribution and seasonality in the Solomon and Coral Seas, *J. Geophys. Res. Oceans*, *119*, 4669–4687, doi:10.1002/2013JC009741.

Jickells, T. D., et al. (2005), Global iron connections between desert dust, ocean biogeochemistry and climate, *Science*, *308*, 67–71.

Karl, D., R. Letelier, L. Tupas, J. Dore, J. Christian, and D. Hebel (1997), The role of nitrogen fixation in biogeochemical cycling in the subtropical North Pacific Ocean, *Nature*, *388*, 533–538.

Karl, D. M., M. J. Church, J. E. Dore, R. Letelier, and C. Mahaffey (2012), Predictable and efficient carbon sequestration in the North Pacific Ocean supported by symbiotic nitrogen fixation, *Proc. Natl. Acad. Sci. U.S.A.*, *109*, 1842–1849.

Kessler, W. S., and S. Cravatte (2013), Mean circulation of the Coral Sea, *J. Geophys. Res. Oceans*, *118*, 6385–6410, doi:10.1002/2013JC009117.

Knapp, A. N., J. Dekaezemacker, S. Bonnet, J. A. Sohm, and D. G. Capone (2012), Sensitivity of *Trichodesmium erythraeum* and *Crocosphaera watsonii* abundance and N_2 fixation rates to varying NO_3^- and PO_4^{3-} concentrations in batch cultures, *Aquat. Microb. Ecol.*, *66*, 223–236.

Labatut, M., F. Lacan, C. Pradoux, J. Chmeleff, A. Radic, J. W. Murray, F. Poitrasson, A. M. Johansen, and F. Thil (2014), Iron sources and dissolved-particulate interactions in the seawater of the western Equatorial Pacific, iron isotope perspectives, *Global Biogeochem. Cycles*, *28*, 1044–1065, doi:10.1002/2014GB004928.

Langlois, R. J., J. Laroche, and P. A. Raab (2005), Diazotrophic diversity and distribution in the tropical and subtropical atlantic ocean, *Appl. Environ. Microbiol.*, *71*(12), 7910–7919.

Lin, I. I., et al. (2011), Fertilization potential of volcanic dust in the low-nutrient low-chlorophyll western North Pacific subtropical gyre: Satellite evidence and laboratory study, *Global Biogeochem. Cycles*, *25*, GB1006, doi:10.1029/2009GB003758.

Luo, Y. W., et al. (2012), Database of diazotrophs in global ocean: Abundances, biomass and nitrogen fixation rates, *Earth Syst. Sci. Data*, *5*(1), 47–106.

Luo, Y. W., I. D. Lima, D. M. Karl, C. A. Deutsch, and S. C. Doney (2014), Data-based assessment of environmental controls on global marine nitrogen fixation, *Biogeosciences*, *11*(3), 691–708.

Maes, C., B. Dewitte, J. Sudre, V. Garçon, and D. Varillon (2013), Small-scale features of temperature and salinity surface fields in the Coral Sea, *J. Geophys. Res. Oceans*, *118*, 426–5438, doi:10.1002/jgrc.20344.

Mague, T., N. Weare, and O. Holm-Hansen (1974), Nitrogen fixation in the North Pacific Ocean, *Mar. Biol.*, *24*, 109–119.

Menkes, C., et al. (2014), Seasonal oceanography from physics to micronekton in the southwest Pacific, *Deep Sea Res., Part II*, doi:10.1016/j.dsr2.2014.10.026.

Moisander, A. M., A. Beinart, M. Voss, and J. P. Zehr (2008), Diversity and abundance of diazotrophs in the South China Sea during intermonsoon, *ISME J.*, *2*(9), 954–967.

Moisander, A. M., T. Serros, R. W. Pearl, A. Beinart, and J. P. Zehr (2014), Gammaproteobacterial diazotrophs and *nif*H gene expression in surface waters of the South Pacific Ocean, *ISME J.*, *8*(10), 1962–1973, doi:10.1038/ismej.2014.49.

Moisander, P. H., R. A. Beinart, I. Hewson, A. E. White, K. S. Johnson, C. A. Carlson, J. P. Montoya, and J. P. Zehr (2010), Unicellular cyanobacterial distributions broaden the oceanic N_2 fixation domain, *Science*, *327*(5972), 1512–1514.

Moisander, P. H., R. F. Zhang, E. A. Boyle, I. Hewson, J. P. Montoya, and J. P. Zehr (2011), Analogous nutrient limitations in unicellular diazotrophs and *Prochlorococcus* in the South Pacific Ocean, *ISME J.*, *6*(4), 733–744.

Montoya, J., C. Holl, J. Zehr, A. Hansen, T. Villareal, and D. G. Capone (2004), High rates of N2 fixation by unicellular diazotrophs in the oligotrophic Pacific Ocean, *Nature*, *430*, 1027–1032.

Montoya, J. P., M. Voss, P. Kaehler, and D. G. Capone (1996a), A simple, high-precision tracer assay for dinitrogen fixation, *Appl. Environ. Microbiol.*, *62*, 986–993.

Montoya, J. P., M. Voss, P. Kahler, and D. G. Capone (1996b), A simple, high-precision, high-sensitivity tracer assay for N_2 fixation, *Appl. Environ. Microbiol.*, *62*(3), 986–993.

Moutin, T., N. Van Den Broeck, B. Beker, C. Dupouy, P. Rimmelin, and A. LeBouteiller (2005), Phosphate availability controls Trichodesmium spp. biomass in the SW Pacific ocean, *Mar. Ecol. Prog. Ser.*, *297*, 15–21.

Olson, E. M., D. J. McGillicuddy, G. R. Flierl, C. S. Davis, S. T. Dyhrman, and J. B. Waterbury (2015), Mesoscale eddies and *Trichodesmium* spp. Distributions in the Southwestern North Atlantic, *J. Geophys. Res. Oceans*, *120*, 4129–4150, doi:10.1002/2015JC010728.

Raimbault, P., and N. Garcia (2008), Evidence for efficient regenerated production and dinitrogen fixation in nitrogen-deficient waters of the South Pacific Ocean: Impact on new and export production estimates, *Biogeosciences*, *5*(2), 323–338.

Raven, J. A. (1988), The iron and molybdenum use efficiencies of plant growth with different energy, carbon and nitrogen source, *New Phytol.*, *109*, 279–287.

Riemann, L., H. Farnelid, and G. F. Steward (2010), Nitrogenase genes in non cyanobacterial plankton: Prevalence, diversity and regulation in marine waters, *Aquat. Microb. Ecol.*, *61*(3), 235–247.

Sarthou, G., A. Baker, J. Kramer, P. Laan, A. Laës, S. Ussher, E. Achterberg, H. J. W. de Baar, K. R. Timmermans, and S. Blain (2007), Influence of atmospheric inputs on the iron distribution in the subtropical northeast Atlantic Ocean, *Mar. Chem.*, *104*, 186–202.

Shiozaki, T., K. Furuya, T. Kodama, S. Kitajima, S. Takeda, T. Takemura, and J. Kanda (2010), New estimation of N_2 fixation in the western and central Pacific Ocean and its marginal seas, *Global Biogeochem. Cycles*, *24*, GB1015, doi:10.1029/2009GB003620.

Shiozaki, T., T. Kodama, and K. Furuya (2014), Large-scale impact of the island mass effect through nitrogen fixation in the western South Pacific Ocean, *Geophys. Res. Lett.*, *41*, 2907–2913, doi:10.1002/2014GL059835.

Slemons, L. O., J. W. Murray, J. Resing, B. Paul, and P. Dutrieux (2010), Western Pacific coastal sources of iron, manganese, and aluminum to the Equatorial Undercurrent, *Global Biogeochem. Cycles*, *24*, GB3024, doi:10.1029/2009GB003693.

Sohm, J. A., and D. G. Capone (2006), Phosphorus dynamics of the tropical and subtropical north Atlantic: *Trichodesmium* spp. versus bulk plankton, *Mar. Ecol. Prog. Ser.*, *317*, 21–28.

Sohm, J. A., E. A. Webb, and D. G. Capone (2011a), Emerging patterns of marine nitrogen fixation, *Nat. Rev. Microbiol.*, *9*(7), 499–508.

Sohm, J. A., B. R. Edwards, B. G. Wilson, and E. A. Webb (2011b), Constitutive Extracellular Polysaccharide (EPS) production by specific isolates of *Crocosphaera watsonii*, *Front. Microbiol.*, *2*, 229, doi:10.3389/fmicb.2011.00229.

Thompson, A., B. J. Carter, K. Turk-Kubo, F. Malfatti, F. Azam, and J. P. Zehr (2014), Genetic diversity of the unicellular nitrogen-fixing cyanobacteria UCYN-A and its prymnesiophyte host, *Environ. Microbiol.*, *16*, 3238–3249.

Thompson, A. W., R. A. Foster, A. Krupke, B. J. Carter, N. Musat, D. Vaulot, M. M. M. Kuypers, and J. P. Zehr (2012), Unicellular cyanobacterium symbiotic with a single-celled eukaryotic alga, *Science*, *337*(6101), 1546–1550.

Turk-Kubo, K. A., M. Karamchandani, D. G. Capone, and J. P. Zehr (2013), The paradox of marine heterotrophic nitrogen fixation: Abundances of heterotrophic diazotrophs do not account for nitrogen fixation rates in the Eastern Tropical South Pacific, *Environ. Microbiol.*, doi:10.1111/1462-2920.12346.

Villareal, T. A. (1991), Nitrogen-fixation by the cyanobacterial symbiont of the diatom genus *Hemiaulus*, *Mar. Ecol. Prog. Ser.*, *76*(2), 201–204.

Voss, M., H. W. Bange, J. W. Dippner, J. J. Middelburg, J. P. Montoya, and B. Ward (2013), The marine nitrogen cycle: Recent discoveries, uncertainties and the potential relevance of climate change, *Philos. Trans. R. Soc., B*, *368*(1621), doi:10.1098/rstb.2013.0121.

Zehr, J. P., M. T. Mellon, and S. Zani (1998), New nitrogen-fixing microorganisms detected in oligotrophic oceans by amplification of nitrogenase (*nif*H) genes, *Appl. Environ. Microbiol.*, *64*, 3444–3450.

Zehr, J. P., J. B. Waterbury, P. J. Turner, J. P. Montoya, E. Omoregie, G. F. Steward, A. Hansen, and D. M. Karl (2001), Unicellular cyanobacteria fix N_2 in the subtropical North Pacific Ocean, *Nature*, *412*, 635–638.

Zehr, J. P., S. R. Bench, E. A. Mondragon, J. McCarren, and E. F. DeLong (2007), Low genomic diversity in tropical oceanic N_2-fixing cyanobacteria, *Proc. Natl. Acad. Sci. U.S.A.*, *104*(45), 17,807–17,812.